BUS-STOP SHELTERS – IMPROVED SAFETY
(Phases 1 and 2)

Chris Turnbull-Grimes
Wayne A. Charlie
Richard M. Gutkowski
Jeno Balogh

Colorado State University
Fort Collins, Colorado

July 2010

Disclaimer

The contents of this report reflect the work of the authors, who are responsible for the facts and the accuracy of the information presented. This document is disseminated under the sponsorship of the Mountain-Plains Consortium in the interest of information exchange. The U.S. Government assumes no liability for the contents or use thereof.

ABSTRACT

This research was undertaken to 1) design and construct a wall and basic subassembly of an emergency storm shelter comprised entirely of wood that could resist a "missile" (15 lb [6.8 kg], 12-ft [3.66 m] long 2x4 from FEMA 361 specifications) impact at 100 mph (161 km/h) (KE_{Impact} = 3657 ft-lbs [4959 J]) or multiple impacts (not required by FEMA 361) at 80 mph (129 km/h) (KE_{Impact} = 2340 ft-lbs [3173 J]); 2) study the difference in impact response for various specimen configurations, angles of impact, and support conditions; and 3) compare results for impact tests to static tests. Fifty-six impact tests were completed with the missile impacting the specimens at velocities between 63 mph and 116 mph (101 km/h and 187 km/h). High speed video was taken of many of these tests in which velocity at impact, deflection, and time of impact could be determined. Previous research suggested that the ultimate strength at a 0.001-second load duration could be as much as 165% of that at a 10-minute load duration. Although strength was not able to be measured in the impact tests, the kinetic impact energy absorbed by the specimen was able to be calculated. Additionally, three specimens were statically loaded for comparison with these tests. Specimen modifications to increase flexibility significantly increased the ability of the specimen tested to resist impact loading. This was done by constructing a thin, layered specimen to act like netting and adding a polystyrene backing between the specimen and the support system. Additionally, the specimens and their support systems under impact loading were able to withstand a kinetic impact energy 373% to 698% of energy stored at the elastic limit of the statically loaded systems and 250% to 570% of the energy stored in the statically loaded specimen at failure.

TABLE OF CONTENTS

LIST OF FIGURES

LIST OF TABLES

DEFINITION OF TERMS

AOI (Angle of Impact): The angle at which the missile strikes the specimen.

Corrected Deflection: The actual deflection at the point of measurement with a string gauge (potentiometer). This is different from the measured deflection from the string gauge, which will have been provided with a correction factor after calibration has taken place prior to use.

Firing Pressure: The pressure at which the front chamber of the cannon is loaded so as to provide sufficient velocity of the missile (varies, though is ~320 PSI for 120 mph).

Global Deflection: The maximum deflection after the edges of the specimen have been displaced. This will always be larger than the local deflection.

Impact Load Test: Test in which a missile was fired at the specimen. The duration of load is less than 0.1 seconds.

Local Deflection: The maximum deflection at which the edges of the specimen have not been displaced.

M1, M2 (Method of Fastener Installation: "Method 1" (Figure 2.20) and "Method 2" (Figure 2.21), respectively.

Missile: A twelve foot long 2x4 with five feet from one end modified so as to fit in the barrel of the cannon.

Missile Reflection: The movement of the missile away from the specimen after impact; the missile bouncing off of the specimen.

Projectile: A 2.75" diameter, 2" long aluminum or plastic rod that is placed in the barrel between the missile and the check valve so as to create a seal that the missile is unable to do. If the projectile is not placed in the barrel, the resulting velocity will not be the design velocity as the majority of the pressure is released around the missile, rather than behind it.

Specimen: A wall or subassembly of varying components to be used for testing.

Specimen Configurations: Refers to orientation of boards.

- **SV:** Strong axis bending, vertically placed
- **SH:** Strong axis bending, horizontally placed
- **WV:** Weak axis bending, vertically placed
- **WH:** Weak axis bending, horizontally placed

Stabilizing Pressure: The pressure at which the rear chamber of the cannon provides for a counterbalance to build the necessary firing pressure (~150 PSI). This pressure is dropped to zero (gauge pressure) to fire the projectile.

Static Load Test: Test in which the specimen was ramp loaded using an actuator. The deflection is measured using potentiometers.

T_{Impact} (Duration of Load): Measured from high speed video for impact tests. For static tests, calculated as the quotient of the deflection at the elastic limit (inches) divided by the loading rate (inches/minute).

Withdrawal Capacity: The ability of the fastener (screw, nail) to resist being pulled/pushed from the specimen.

EXECUTIVE SUMMARY

Bus-stop shelters (school and public transit) typically provide, at best, only limited reduction to exposure to rain, snow, wind, and direct sunlight. Most shelters provide little or no reduction in potential injury from severe storms (wind, wind generated missiles, or hail) or vehicle impacts. The ongoing research effort involves the evaluation of potential bus-stop shelter designs, including a timber-based design, to evaluate and upgrade the impact resistance of bus-stop shelters. The long-term research objectives are to design, construct, and test a prototype timber bus-stop shelter capable of providing improved safety to occupants from vehicle impacts, hail, and windstorm (e.g., hurricane) generated debris.

This report describes a comprehensive physical testing program that involved:

a) Impact load tests of small preliminary specimens to develop the impact test procedures,
b) Testing a variety of prototype single-wall sub-assemblies using procedures and a dimension lumber missile prescribed in FEMA 361 and ASTM E 1886 and E 1996 test methods for impacts from hail and hurricane and tornado generated debris, and
c) Impact load tests on specimens comprised of two orthogonally connected walls stiffened at top and bottom to simulate the overall stiffness of a four-sided unit.

Fifty-six impact tests were completed with the missile impacting the specimens at velocities between 63 mph and 116 mph (101 km/h and 187 km/h). A standardized cannon and projectile were used and the variability of the potential angle of attack was accomplished by fixing specimens to an angularly adjustable base support. The projectile was a modified 15 lb [6.8 kg], 12-ft [3.66 m] long 2x4 (consistent with FEMA 361 specifications). Although an official performance test consists of only firing on one specimen, some multiple shots were considered. The work done to date has led to instances of stopping or repelling projectiles successfully, but infrequently and inconsistently.

The successful outcomes indicate that repelling or stopping the missile involves absorption of and/or release of kinetic energy upon impact. A buffer backing material improves absorption, while freedom of the base to displace releases energy. So both means were investigated at incrementally increased velocities so as to make adjustments and work toward stopping or repelling missiles consistently at hurricane level velocities – but that consistency is yet to be achieved. Specimen modifications made to incorporate specimen flexibility significantly increased the ability of the specimen tested to resist impact loading. This was done by constructing a thin, layered specimen to act like netting and adding a polystyrene backing between the specimen and the support system.

High speed video was taken of many of these tests in which velocity at impact, deflection, and time of impact could be determined. Although strength was not able to be measured in the impact tests, the kinetic impact energy absorbed by the specimen was calculated. The high speed digital camera imaging provides records of the impact events in a time record. These records provide data for development of a suitable structural analysis model needed to simulate the dynamic impact response of potential whole structure specimens, evolve a prototype system, and conduct full-scale impact load tests on the prototype.

1. INTRODUCTION

1.1 Problem Statement

The long-term objective of ongoing research at Colorado State University (CSU) is to develop a bus shelter containing ten to twenty people able to sustain the impact loads from tornadoes and hurricanes, which the research described herein is the result of the first two phases. Phase 1 was conducted to develop a technique for and conduct pilot tests to achieve desired test velocities and visually record them. Phase 2 was conducted to (a) design an all wood wall "specimen" that could withstand impact loads set forth by FEMA 361 specifications, (b) observe how key components (specimen geometry, fastener type and arrangement, loading variations, and support configurations) affect the behavior of the specimen under impact loading, and (c) observe how materials perform under very short duration, high impact loadings.

Throughout the world, hurricanes and tornadoes cause billions of dollars of damage to homes and businesses and cause a tremendous loss of life. In the United States alone, tornadoes account for an average of 89 deaths per year; hurricanes can cause even more fatalities, as Hurricane Katrina reminded the world, taking the lives of 1,836 people (FEMA 361). In these events, significant damage to property and, more importantly, loss of human life occurs from the flying debris ("missiles") produced by the severe winds. As a result, safe rooms (built-up enclosures in residences, offices, schools, etc.), safe shelters (structures to provide emergency protection for pedestrian access in a community), and safe storage facilities for hazardous materials have been developed to combat the loss of life from this flying debris. Usually these shelters are designed using a combination of metal and concrete, but this results in high costs and a difficulty in readily expanding these for use in larger structures, such as hospitals, bridges, and other important pieces of infrastructure. Shelter walls that include wood in their design have been constructed at Texas Tech University (TTU 2003), but the wood is generally used as a sheeting material instead of the primary structural component in successful tests.

1.2 Literature Review

1.2.1 Effect of Load Duration

Elmendorf (1916) performed impact tests on 1 in. (25 mm) by 1 in. (25 mm) by 1 ft. long (30 cm) span Douglas-fir specimens. Elmendorf determined that the modulus of rupture for a 15 millisecond loading was approximately 175% of the conventional 5 min. static load tests. Liska (1950) compared ultimate strength failure loading duration for small, clear Douglas-fir beams (one inch [25mm] by 1 in. [25 mm] by 1 ft. [30 cm] long span). The data exhibited significant scatter but generally showed an increase in the ultimate strength as the time of loading to failure decreased though, as Figure 1.1 shows, Liska estimated a linear increase in strength with load duration decrease. The strength increase was in ratio to the strength used for design at 10 min. (600 seconds) load duration,[1] as shown in Figure 1.1.

Wood (1951) performed 126 bending tests on one inch (25 mm) by 1 in. (25 mm) by 1 ft. (30 cm) span Douglas-fir specimens with load durations ranging from five minutes to five years. Figure 1.2 plots a summary of Wood's data for ultimate bending load capacity for the aforementioned load durations. Figure 1.2 also plots the straight line of best fit from Figure 1.1, which is labeled as "Trend of Data in

[1] A 10-min. load duration was used for the base strength as opposed to the 5-min. load duration by Elmendorf since the accepted duration for design strength changed in the period between the two studies.

Rapid Loading." Wood estimated that timber exhibits ultimate bending strength of up to 165% of 7.5 min.[2] strength during one millisecond load durations.

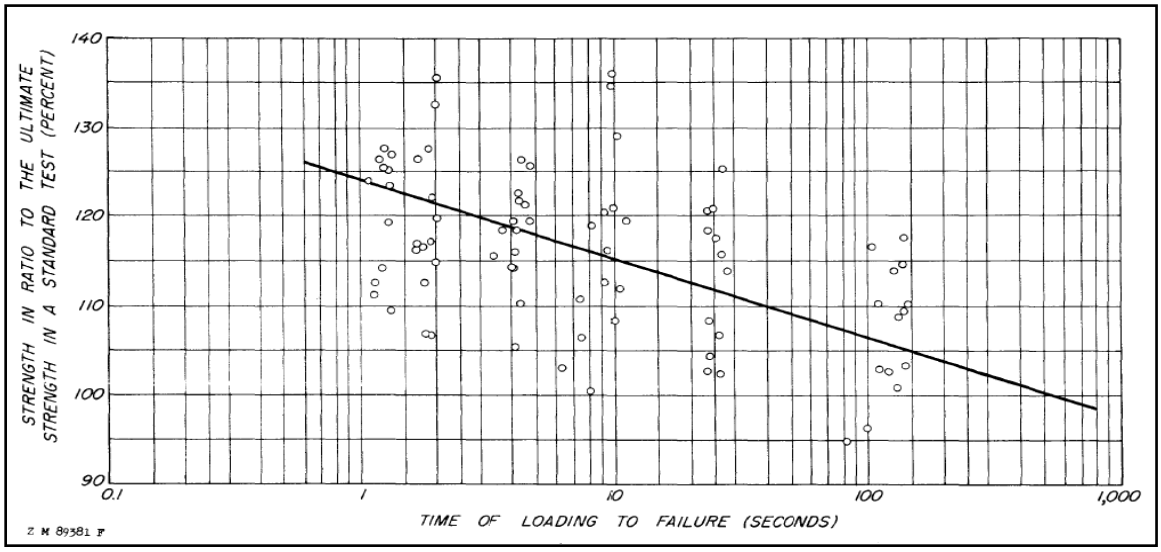

Figure 1.1 Ultimate Strength Ratio vs. Duration of Bending Load (Liska 1950)

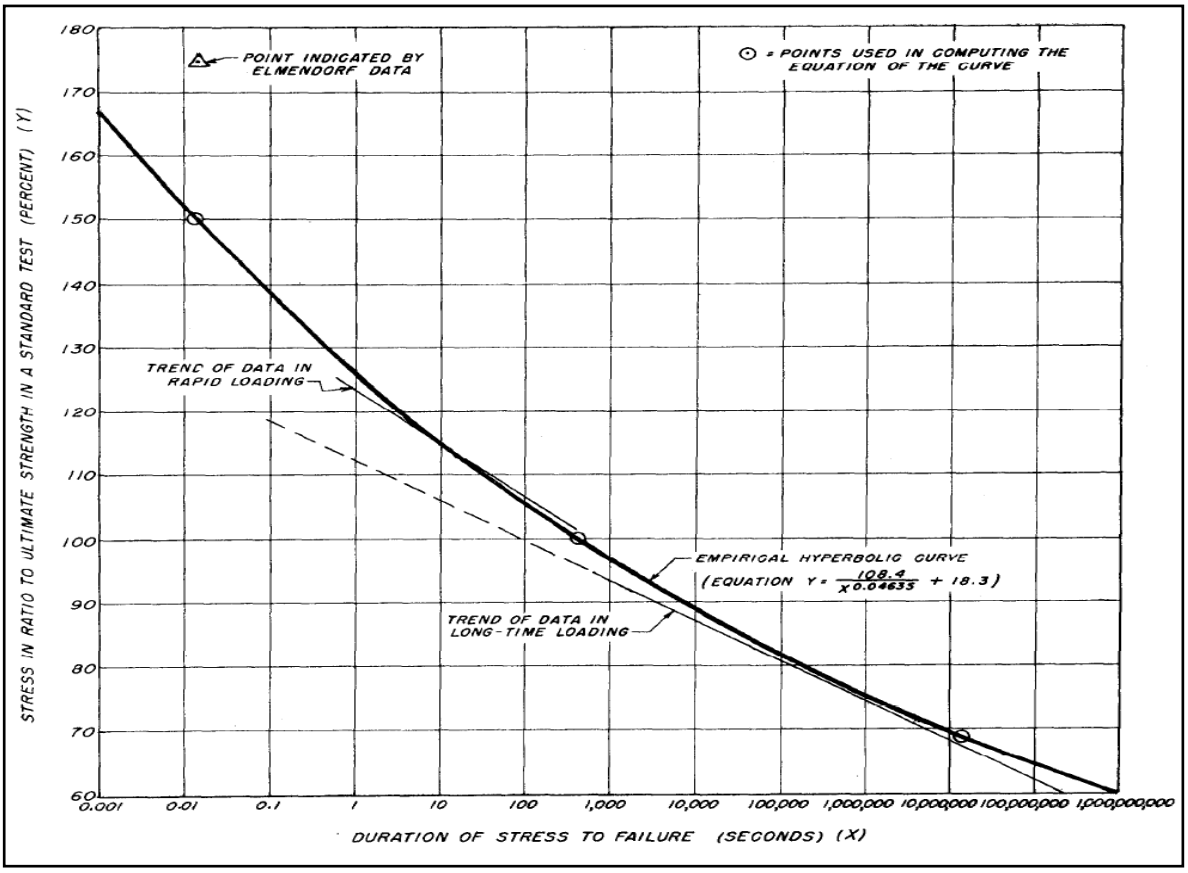

Figure 1.2 Ultimate Strength Ratio vs. Duration of Bending Stress (Wood 1951)

[2] Figures 1.1 and 1.2 refer to the 7.5 min. load duration as the "Standard Test."

These studies provided only one data point for loads with duration less than 0.5 seconds and no data for loadings with durations less than 0.01 seconds. Thus, in Figure 1.2 the plotted curve is an extrapolation below 0.01 seconds. For testing hurricane and tornado debris, impact only occurs for a few thousandths of a second, so additional testing is needed to develop accurate wood structure design criteria for impact loads.

Two other pertinent studies have been performed with an array of results ranging from a large strength increase to a small strength decrease at smaller durations of impact. Buchar and Adamik (2001) performed impact tests using a small cylindrical projectile and small cylindrical birch and spruce specimens; they found an impact tensile strength as much as 263% of the static tensile strength with a projectile impact velocity as high as 500 mph (220 m/s). Jansson (1999) performed drop tests in which he concluded that the wood strength actually decreases with a decrease in load duration. The wide variation in results necessitates more testing, though the research provided herein does not attempt to determine wood strength increases.

1.2.2 FEMA 361 Impact Load Testing Criterion

In order to standardize the testing methods to approve tornado and hurricane safe shelters, the Federal Emergency Management Agency (FEMA) developed the FEMA 361 regulations, which set forth standards and recommended practices for the design and construction of such shelters. On the Fujita Tornado Scale (NOAA 2007), a Category 5 tornado develops a 250 mph (403 km/h) design wind speed, which can result in a 15 lb (6.8 kg) missile being projected at a velocity of 100 mph (161 km/h) with a kinetic energy at impact of 3657 ft-lbs (4959 J). Due to extensive use of dimensioned lumber nominal 2x4s for building materials, FEMA concluded that this is the most likely type of debris to cause extensive damage. Additionally, FEMA concluded that the vertical projectile wind design velocity should be two-thirds of the horizontal projectile wind speed. Standardized test methods are also given in ASTM E 1886 and E 1996.

Figure 1.3 presents FEMA standards for testing of shelter with a chart of the predominant wind types, their design speeds, and the wind zone of the United States that experiences each wind type. Appendix A provides a map of the United States with each wind zone designation. It was believed that though the possibility of multiple impacts occurring during a hurricane was miniscule, it would be useful to repeat the impact test to ensure the safety of the inhabitants inside the shelter.

WIND ZONE	PREDOMINANT WIND TYPE	DESIGN WIND SPEED	MISSILE SPEED AND DIRECTION
I	Tornado & Hurricane	130 mph	80 mph Horizontal 53 mph Vertical
II	Tornado & Hurricane	160 mph	84 mph Horizontal 56 mph Vertical
III	Tornado	200 mph	90 mph Horizontal 60 mph Vertical
IV	Tornado	250 mph	100 mph Horizontal 67 mph Vertical

Figure 1.3 FEMA 361 Standards for Missile Testing of Shelters (FEMA)

1.2.3 Impact Studies

Researchers at TTU have examined the ability of various wall configurations to resist missile impacts at velocities up to 150 mph (242 km/h). One of the test configurations was a specimen comprised of four layers of 3/4 in. (19 mm) thick plywood. The plywood was then rigidly fastened to two 2x4 studs using screws. The fastener configuration was not provided, but Table A7 of the Summary Report of Debris Impact Testing (TTU) shows that this specimen type was tested at velocities ranging from 85 to 100 mph (137 to 161 km/h) with the missile fully penetrating the wall specimen in each test. The missile was a 12 ft (3.7 m) long, 15 lb (6.8 kg) nominal 2x4 and the impact energies ranged from 3657 to 5091 ft-lb (4959 to 6903 J). The specimen was estimated to have a threshold of less than 82 mph (132 km/h).

The Engineered Wood Association sponsored impact testing of an all wood 4x4 (1.22 m x 1.22 m) wall using "Lock-Deck" glulam deck planks. The planks were nominally sized at 4x6 (actual size = 3.66 in. x 5.25 in. [93 mm x 133 mm]), which consisted of five offset laminations to create a "double tongue and groove system" (Zylkowski) and structural 3M 5200 adhesive was placed in the tongue and grooves. Studs were spaced at 12 in. (0.30 m) on center and were connected to the planks using 6 in. (152 mm) long, 1/4 in. (6.35 mm) diameter lag screws. Two impact tests using the standard missile at 100 mph were performed on the wall. The first one stopped the missile, though penetration occurred (the amount was not specified) and the second entirely passed through the wall.

1.3 Research Objectives

The objectives of the research described herein were to:

1. Design and test a wall and basic subassembly of an emergency shelter manufactured solely of wood, with exception given to fasteners and connectors. Ideally, the structure would be strong enough to resist both tornado impact tests (single test at 100 mph [161 km/h]) and hurricane impact tests (multiple tests at 80 mph [129 km/h]).

2. Study the differences in impact response (ability to pass test) for various
    a. specimen configurations,
    b. fastener types and distributions, and
    c. angles of impact.

3. Compare results for impact tests versus traditional static load testing on specimens.

1.4 Research Method

1.4.1 Impact Load Testing

In order to fire the missile at the required velocities, researchers at CSU used of a cannon with two chambers pressurized with nitrogen and a shaft long enough to encase approximately five feet (1.5 m) of the wood missile, resulting in the need to modify one end of the standard FEMA 2x4 missile by trimming one end to a width of 2.0 in. (51 mm) (Figure 1.4). With the modifications, the missile weighs approximately 11 lb. (5.0 kg), resulting in a necessary velocity of 117 mph (188 km/h) to achieve 3,657 ft.-lb. (4959 J) of kinetic energy upon impact equivalent to that of the FEMA specified 15 lb. (6.8 kg) 2x4 missile traveling at 100 mph (161 km/h). Both chambers are pressurized initially, and then the stabilizing pressure is released in rear chamber. This causes the front chamber to rapidly open a check valve that accelerates the missile using the firing pressure. Eight calibration tests were performed by varying the firing pressure and calculating the velocity of the missile upon exiting the cannon barrel using the method

described in Section 2.2.1. This velocity is slightly more than at impact, but the difference was considered to be negligible.

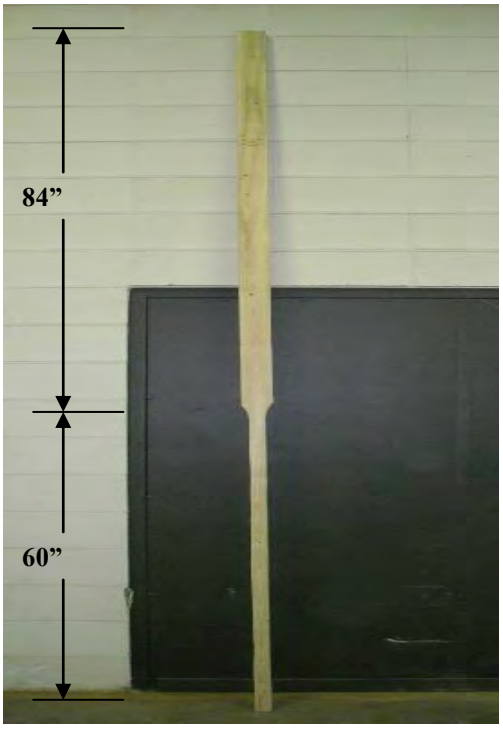

Figure 1.4 Modified Wood Missile

A facility was developed to test various sizes and configurations of walls at several angles. Additionally, high speed camera footage was used to determine deflections and impact times for the testing.

1.4.2 Static Load Testing

A static test was developed using a nominal 4x4 modified at the end to the cross-sectional size of a 2x4 to transfer the load from the load cell to the specimen (Figure 1.5) that supported the specimen with similar edge conditions to the specimens in the impact loading test setup. The purpose of this testing was to observe the response of a specific specimen type under ramp loading, which has substantially longer load durations than the impact tests.[3]

[3]The variation in structural responses between the two tests is expected and of importance.

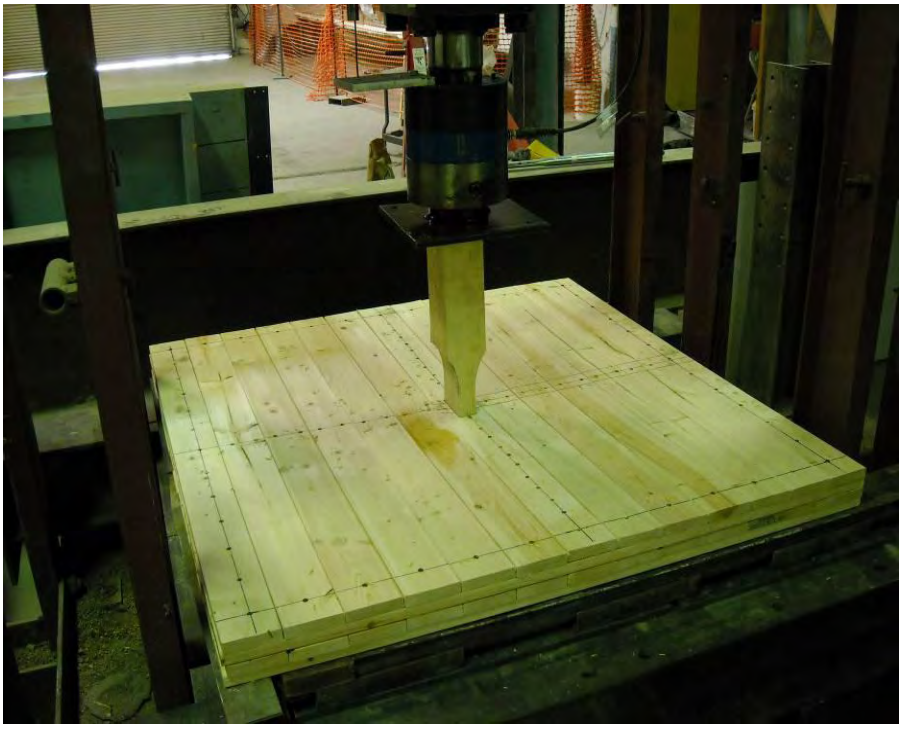

Figure 1.5 Isometric View Diagram of Static Load Test

1.4.3 Impact Loading Characteristics

The magnitude of the impact loading was obtained using the impulse/momentum relationship rearranged to calculate force (Equation 1.1), assuming the missile is fully stopped. Equation 1.2 provides for the calculation of the missile's kinetic energy at impact. Equation 1.3 (Kolsky 1963, Richart 1970) provides for the calculation of the compression wave velocity. This is the velocity at which the force travels from one end of the missile to the other and back after impact. The force-compression wave velocity relationship is expressed by Equation 1.4 (Rinehart 1975). Additionally, T_{max} is the maximum time (assuming a fully rigid wall specimen) in which it takes the peak stress to travel from end to end of the missile and back resulting in missile reflection (the missile moving back away from the specimen after impact), as given by Equation 1.6 (Timoshenko 1970).

$$F = \frac{m * v}{\Delta t} \qquad \text{(Equation 1.1)}$$

Where: F = Impact Force (lbs [N])
m = Missile Mass (slugs [kg])
v = Change in Velocity (ft/sec [m/sec])
Δt = Impact (sec)

$$KE = \frac{1}{2} m v^2 \qquad \text{(Equation 1.2)}$$

Where: KE = Kinetic Energy (ft-lbs [Joules])
v = Missile Velocity (ft/sec [m/sec])

$$c = \sqrt{\frac{E}{\rho}} \qquad \text{(Equation 1.3)}$$

Where: c = Compression Wave Velocity (ft/sec [m/sec])

E = Modulus of Elasticity (lb/ft^2 [kPa])

ρ = Mass Density (slugs/ft^3 [kg/m^3])

$$F = v * \rho * c * A \qquad \text{(Equation 1.4)}$$

Where: A = Missile Cross Section Area (ft^2 [m^2])

$$T_{max} = \frac{2 * L}{c} \qquad \text{(Equation 1.5)}$$

Where: T_{max} = Maximum Time for Peak Stress (sec)

L = Missile Length (ft [m])

It is of interest to examine the consequence of impact loads at the extreme case of a "rigid" specimen and support system. Tables 1.1a and 1.1b show the properties of the missile pertinent to the compression wave velocity for both the modified missile and the FEMA 361 missile. Table 1.2 shows the calculations for the kinetic impact energy, the impact force, and the time of impact. It is important to note that the calculations shown here are entirely independent of the actual loads on the specimens during impact testing. These calculations are only to represent the impact force and time for the missile reflection for entirely rigid specimens, which would result in a force of 84 kips (374 kN) for the modified missile at 117 mph (188 km/h), 60 kips (267 kN) for the modified missile at 83 mph (134 km/h) (for later comparison to actual tests) and 72 kips (320 kN) for the FEMA 361 missile at 100 mph (161 km/h). All calculations are shown in both standard and metric units. The missile weight was measured after missile modification and the properties for the Grade #2 Southern Pine used were obtained from National Design Specification Table 4B (AFPA 2001).

Table 1.1a Missile Properties

Missile	Length		Weight		Mass		Modulus of Elasticity	
	ft	m	lbs	kN	slugs	kg	psf	kPa
Modified	12	3.66	11	0.05	0.34	4.99	1.585E+08	7.590E+06
FEMA 361	12	3.66	15	0.07	0.47	6.81	1.585E+08	7.590E+06

Table 1.1b Missile Properties (continued)

Missile	Mass Density		2x4 Cross-Section		Comp. Wave Vel. (Eq 1.4)	
	sl/ft^3	kg/m^3	ft^2	m^2	ft/s	m/s
Modified	36.83	590	0.0365	0.0034	365.58	113.42
FEMA 361	36.83	590	0.0365	0.0034	365.58	113.42

Table 1.2 Compression Wave Velocity Calculations

Missile	Velocities			Kinetic Energy (Eq 1.3)		Impact Stress = F/A		Impact Force (Eq 1.5)		T_{max} for σ_{peak} (ms) (Eq 1.6)	
	mph	ft/s	m/s	lb-ft	kN-m	ksf	kPa	kips	kN	Standard	Metric
Modified	117	171	52.20	5010	6800	2306	108484	84.08	367.41	65.65	64.49
Modified	83.2	122	37.20	3470	4709	1644	77311	59.92	261.83	65.65	64.49
FEMA 361	100	147	44.70	5010	6800	1975	92899	72.00	314.63	65.65	64.49

2. EXPERIMENTAL INVESTIGATION

2.1 Equipment

2.1.1 Missile Propulsion

A nitrogen powered cannon developed by Veyera (1985) was employed to launch the wood missile. As shown in Figure 2.1, the cannon is approximately six feet (1.8 m) long, with two chambers and a barrel. The cannon is attached to two pressurized nitrogen canisters and, along with the PVC barrel extension, connected to two horizontally and vertically adjustable steel A-frames (Figure 2.2) which permit a wide spectrum of angles and locations of impact. The projectile is placed in the base of the barrel between the missile and the check valve.

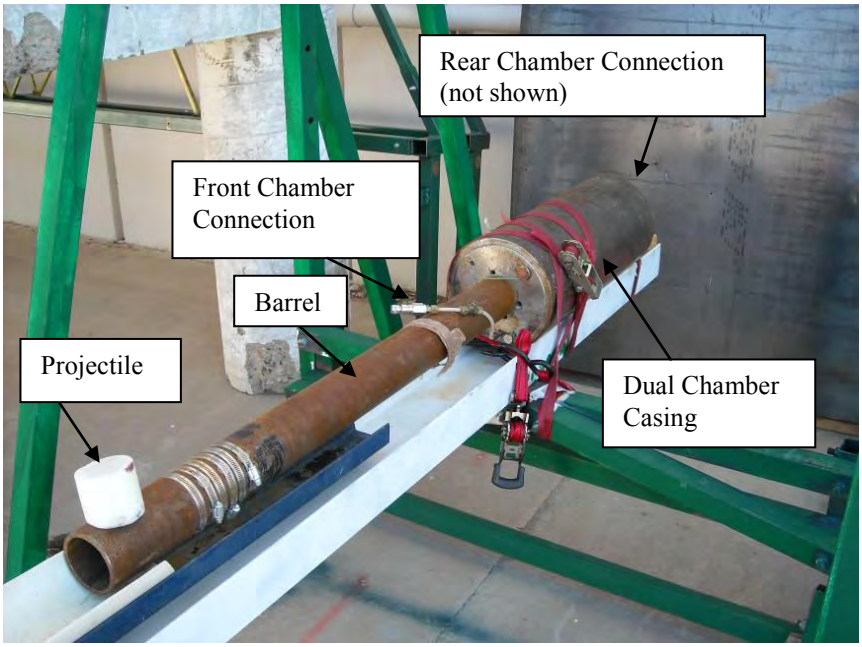

Figure 2.1 Cannon with Projectile

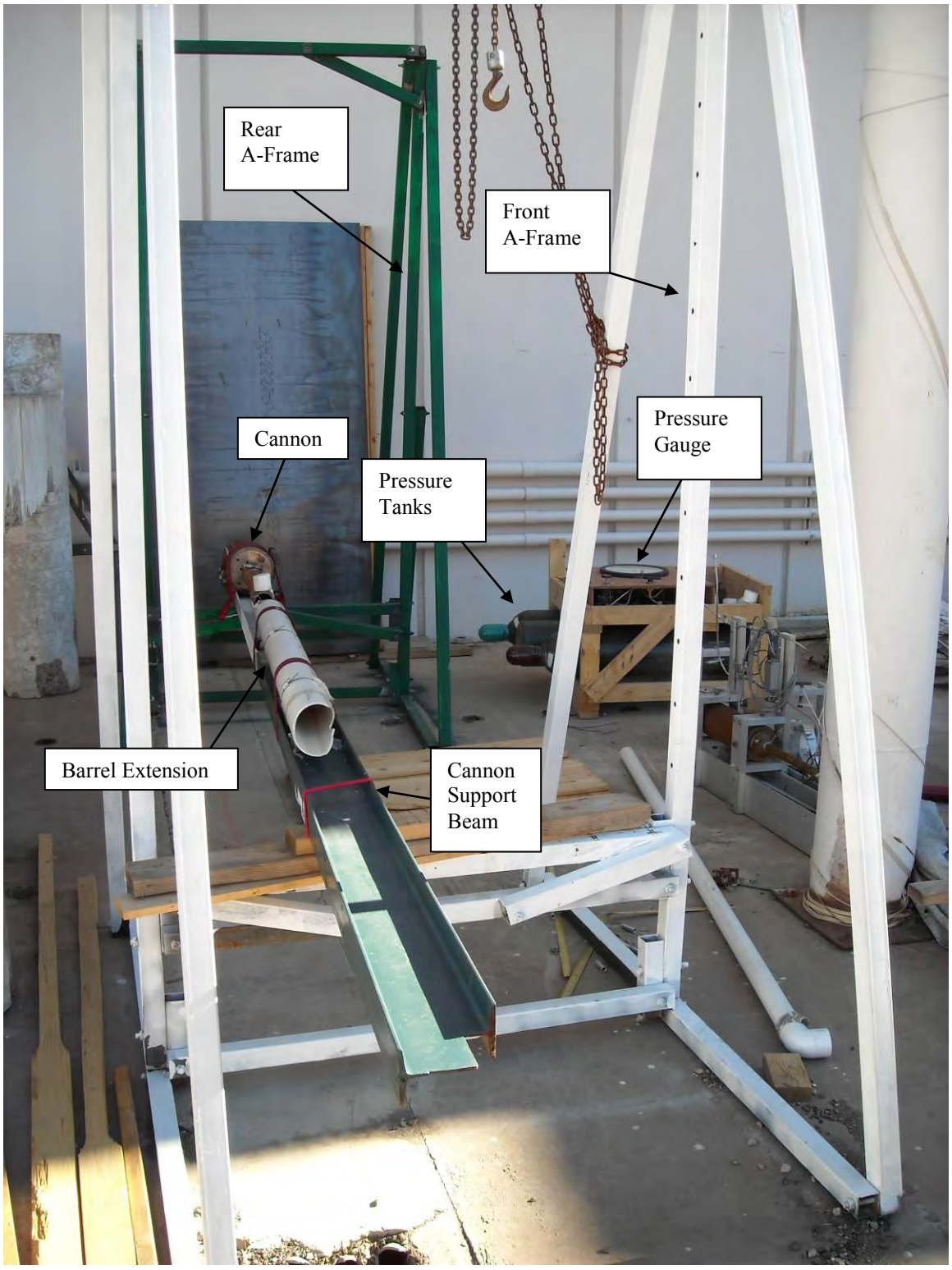

Figure 2.2 Cannon Experimental Test Setup

2.1.2 Specimen Geometries

Specimens of varying sizes and configurations were tested. The specimens also varied as to the components, with specimens being comprised of 2x4; 2x4 and 2x2 combinations; 1x2; or 1x4. In some cases, multiple specimens were constructed in order to test different fastener configurations, angles of impact, and support rigidities along with the need to test multiple specimens of a single configuration.

2.1.3 Impact Load Test Specimen Support

In phase 1, four different specimen support systems were utilized in order to test different facets of the structure design from varying the rigidity of the supports to the testing of the specimens' different impact angles.

Initially, 24 in. x 48 in. (0.61 m x 1.22 m) specimens were tested in a laboratory in a wood enclosure with a wood backing frame rigidly supporting the specimen (Figure 2.3) and a distance of 24 ft (7.3 m) between the end of the cannon barrel and the impact surface of the specimen. It was also desirable to test larger specimens to more accurately represent as-built shelter components. To facilitate progress toward this, the test facility was moved to an outdoor location.

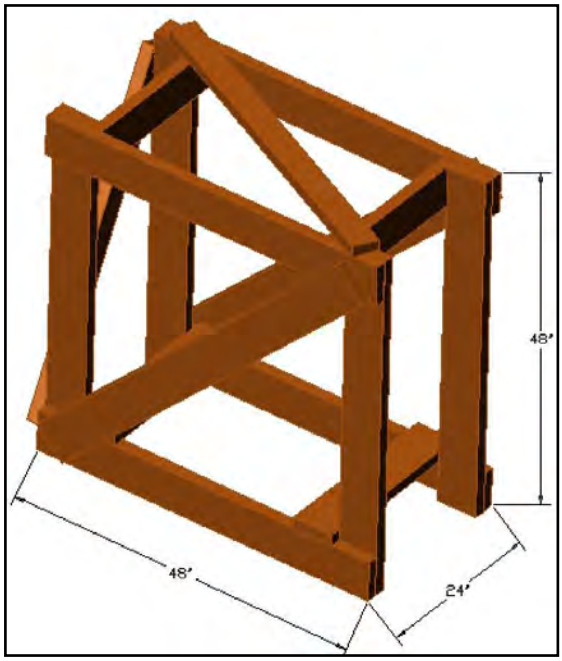

Figure 2.3 Wood Backing Frame

In phase 2, second specimen support system was developed in which a steel backing frame was used instead of wood for additional support strength. It also included a horizontal turntable that allowed for testing of structures with multiple sides and testing various impact angles (Figure 2.4) at a distance of 40 ft (12.2 m) between the end of the cannon barrel and the specimen's impact surface.

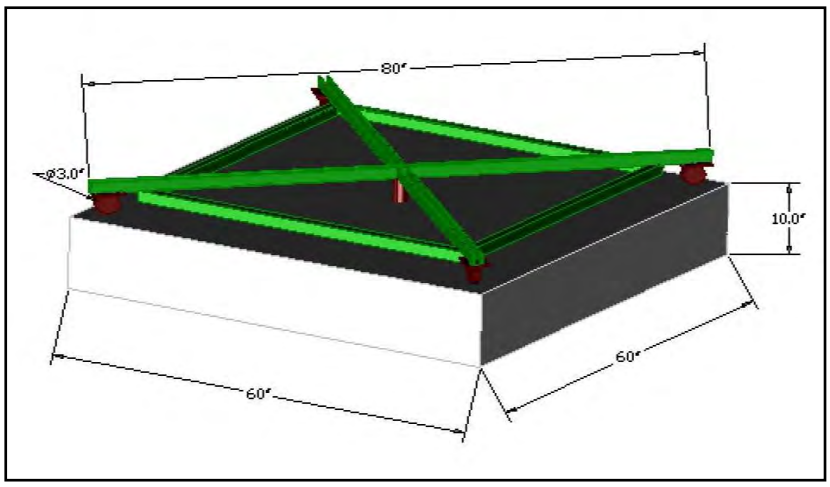

Figure 2.4 Turntable and Concrete Base

A pair of vertical steel A-frames were constructed and attached to the turntable, as shown in Figure 2.5. These frames were adjustable to the width and height of the specimen being tested. This improved test efficiency.

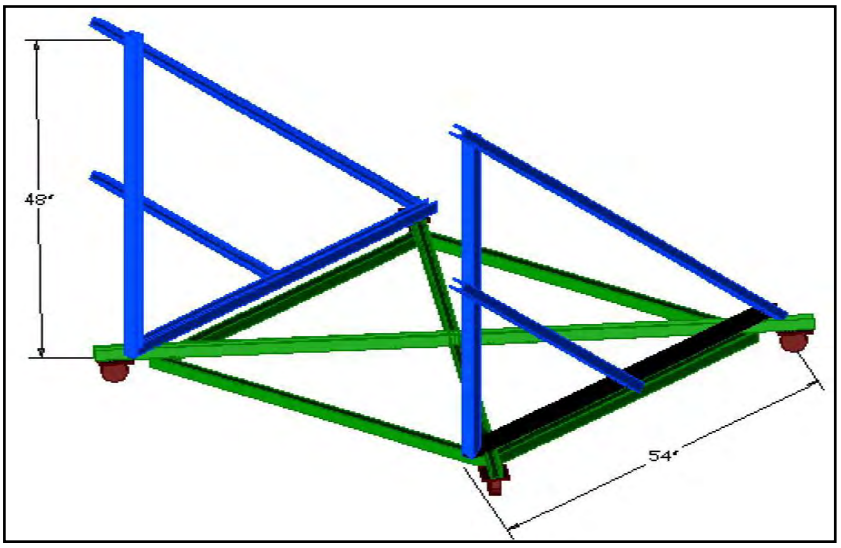

Figure 2.5 Steel Backing Frame Support

A support was desired that was both rigid enough to support the entire impact force while being flexible enough to spread the load throughout the specimen. Testing showed that the steel backing frame support was too rigid for thinner walls. As discussed in Section 1.4.3, supports with higher rigidity would result in larger impact loads. To decrease the load it was necessary to increase the time of impact (Equation 1.2), so a flexible backing support (essentially a "shock absorber") was developed that was placed between the rigid support and the specimen. One inch (25 mm) thick polystyrene Styrofoam was used to achieve this purpose (Figure 2.6).

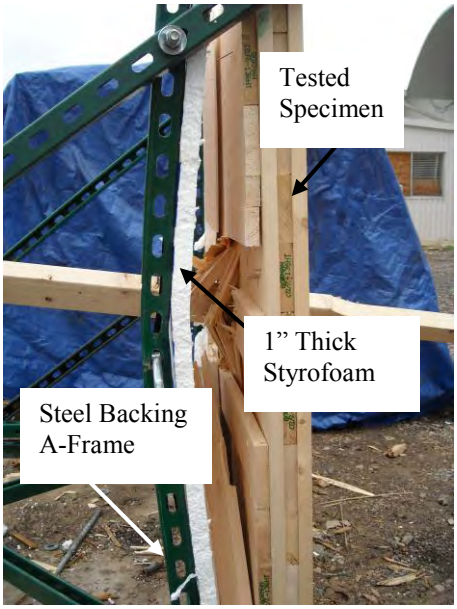

Figure 2.6 Flexible Backing

The fourth method of supporting a specimen was to orthogonally attach two specimens together at right angles using two triangular sections of ¾ in. (19 mm) plywood on top and bottom of the specimens (Figure 2.7). This was done to begin to simulate an actual structure and the support conditions between two walls in the structure. Additionally, a nominal 4x4 wood post was placed at the corner that attached the two specimens, on the opposite side of the firing surface. This structure was attached to the steel turntable and proved to be effective in supporting the specimens.

2.1.3 Static Load Test

A 100 kip (445 kN) MTS actuator was used to perform the static load test. The cylinder was capable of a 6 in. (152 mm) stroke and consisted of a bearing plate at the contact point with the specimen, a load cell, a deflection measurement attachment, and connections to the control unit for deflection, force, and flow valve control (Figure 2.8).

2.1.4 Static Load Test Specimen Support

To simulate the conditions where the structure was self supported (two specimens orthogonally attached), the specimen was placed in a flat position and was vertically supported by rollers on three sides. The rollers were supported on three steel I-beams which were then placed on an existing overhead frame system also comprised of steel I-beams, as shown in Figure 2.8. The overhead frame also supported the actuator.

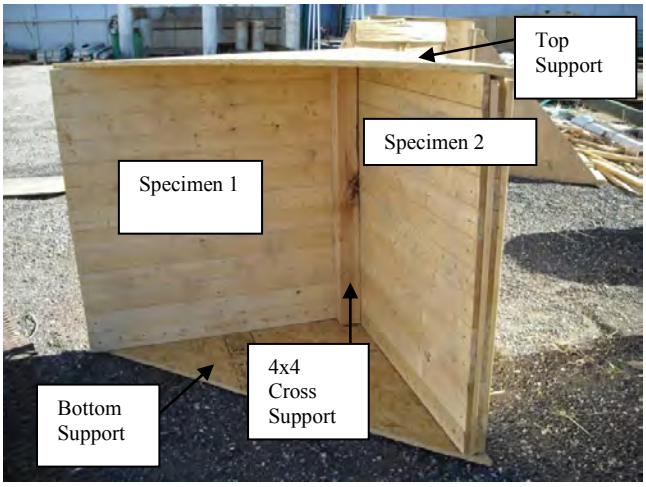

Figure 2.7 Wall Self-Supporting Structure

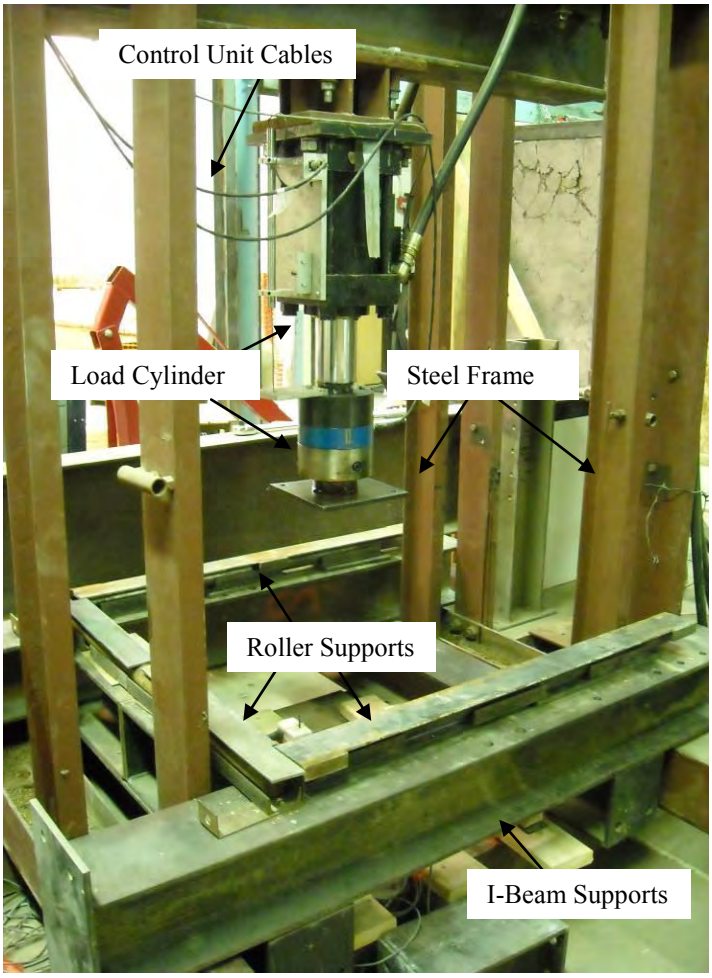

Figure 2.8 Static Loading Specimen Support

2.2 Instrumentation

2.2.1 Projectile Velocity and Impact Test Time Measurement

Multiple methods were used to calibrate and measure the velocity of the missile. First, a Hewlett Packard 5300A timer was employed with accuracy to within a nanosecond (Figure 2.9). The timer system uses two sets of electrodes. Each set is an interconnected pair. The timer is started when the first circuit is broken (i.e., first pair separated) and continues until the second circuit is broken. For the purposes of this testing, the circuit was created by attaching the gator clamps on the electrodes to two nails, running a strip of aluminum foil between the nails, and placing this system at the end of the cannon support beam (Figure 2.10). The circuit would be broken as the projectile cut each piece of aluminum foil. For this test, the distance between the two foil strips was set as 18" (45 cm). Consequently, a reading of 10.23 milliseconds between circuit breaks would indicate a velocity of 100 mph (161 km/h).

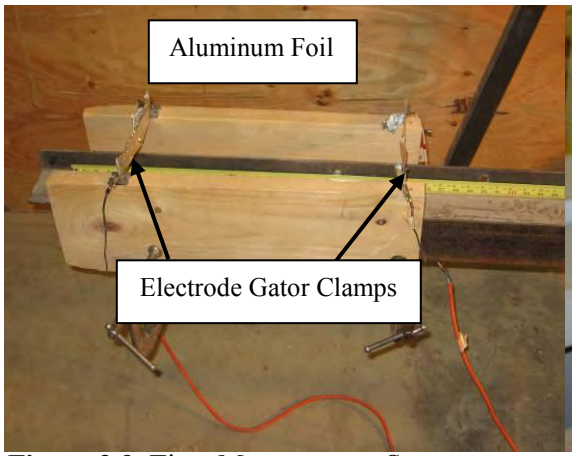

Figure 2.9 Time Measurement Setup

Figure 2.10 HP 5300A Timer

High speed camera footage was utilized to capture the missile events. This was done for multiple reasons. First, it was desired to see how the projectile and the target reacted to the shot in the period of a few milliseconds. Second, the projectile was marked at every 2 in. (51 mm), resulting in the ability to calculate velocity by recording the time durations for it to travel a known distance. Lastly, it was also possible to determine the deflection of the wall at the impact point, as described in Section 2.2.2. The camera used was a Kodak Motion Corder Analyzer PS-110 with RGB CCD that could record at up to 10,000 frames per second, but was used at 3,000 frames per second.

Figure 2.11 Kodak Motion Corder Analyzer PS-110 (Alciatore)

Multiple preliminary test shots were conducted to determine the amount of pressure necessary to obtain the desired velocity of approximately 117 mph (188 km/h) (Section 1.4.1). It was determined that 320 psi (2200 kPa) in the firing chamber would consistently satisfy this requirement. The results from each of these calibration tests are in Appendix B, with the results from the firings upon each specimen.

2.2.2 Impact Load Deflection Measurement

Measurement of the missile impact event was accomplished using high speed video capture with the missile marked at two inch (51 mm) intervals, which are marked in each image in Figure 2.12. Using the first image's scale, the missile velocity was then calculated prior to impact. In Figure 2.12, the top measurement of 0.2577 in. (6.5 mm) is scaled to 2 in. (51 mm).[4] The other measurements are then set to an equal scale. The first two images in Figure 2.12 show the missile prior to impact, while the third image shows the missile at impact. The two distances traveled were combined with the video time intervals to determine missile velocity. The fourth image is the moment of maximum local deflection (maximum deflection before any edge response noticed). The fifth image is the moment of maximum global deflection (maximum overall deflection of specimen). Lastly, the time of impact was able to be measured using the high speed video. It is difference in time between impact and the moment when the missile begins to travel backwards from its original direction.

[4] In AutoCAD, this dimension was measured as 0.2577 in. (6.5 mm). Since it was known that the actual distance was 2.0 in. (51 mm), it was then possible to determine the distance that the missile traveled between frames. Since the high speed camera measured the time, the missile velocity was calculated.

Figure 2.12 Impact Load Deflection Measurement

2.2.3 Static Load Deflection Measurement

To measure the deflection of the specimens, nine string potentiometers were arranged in a 3x3 grid pattern. The potentiometers (Figure 2.13) were placed at 11.25 in. (28.6 cm) spacings (45 in. divided into four sections) and were attached to eye-hooks screwed into the bottom (rear) layer of the specimen. Potentiometers were calibrated before use, and the deflections provided in the results are the corrected deflections.

Figure 2.13 String Gauge Deflection Measurement

2.2.4 Static Load Measurement

The device used to control the static load was an MTS 407 Controller (Figure 2.14). This control unit is capable of controlling the load cylinder through either load or displacement control.[5]

Figure 2.14 Static Load Control

[5] This device was not used for deflection measurement because it would only measure the deflection at the center of the specimen being tested.

2.3 Specimens

Appendix B refers to the various specimens and their configurations used for testing. All specimens used either nominal 1x2s (actual size – 0.75 in. x 1.5 in. [19 mm x 38 mm]), 1x4s (0.75 in. x 3.5 in. [19 mm x 89 mm]), 2x2s (1.5 in. x 1.5 in. [38 mm x 38 mm]), 2x4s (1.5 in. x 3.5 in. [38 mm x 89 mm]) or combinations of them.

2.3.1 Comprised of 2x4s

A series of impact tests were first completed with specimens constructed solely of 2x4s. Two specimens were sized at 4 ft. (1.2 m) wide by 8 ft. (2.4 m) tall and three were sized at 2 ft. (0.6 m) wide by 4 ft. (1.2 m) tall. Table 2.1 shows the various specimen sizes and layer structure. Terms SV and SH refer to the bending about the strong axis with the 2x4 boards aligned vertically or horizontally, respectively (Figure 2.15). Each of the specimens comprised solely of 2x4s was connected with fasteners (screws or ring-shanked nails) at 6 in. centers. For each of the specimens sized 1 ft. x 1 ft. (30 cm x 30 cm), two 1/2 in. (12 mm) diameter, 14 in. (36 cm) long bolts were inserted and connected to the frame. All layers for specimens constructed out of 2x4s were framed by a wider board in order to connect the layers together.

Table 2.1 2x4 Specimen Configurations

Wall Size	1st Layer	2nd Layer	3rd Layer
4'x8'	2x4 - SV	N/A	N/A
4'x8'	2x4 - SV	2x4 - SH	N/A
2' x 4'	2x4 - SV	2x4 - SH	N/A
2' x 4'	2x4 - SH	2x4 - SV	N/A
2' x 4'	2x4 - SH	2x4 -SV	2x4 - SH
1' x 1'	2x4 - SH	2x4 - SV	N/A
1' x 1'	2x4 - SV	2x4 - SH	N/A

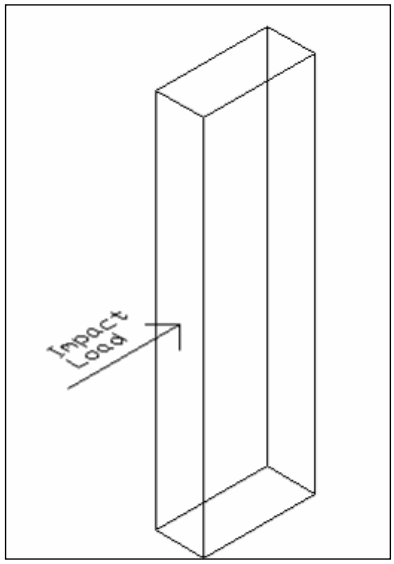

Figure 2.15 Strong Axis Bending

2.3.2 Comprised of 2x4s and 2x2s

Two specimens were constructed from a combination of 2x4s and 2x2s, both sized at 2 ft (0.6 m) wide by 4 ft (1.2 m) tall (Table 2.2). Because 2x2s are square, they are only described as either H or V, depending on the direction that they were aligned: horizontal or vertical, respectively. All specimens comprised of 2x4s and 2x2s were attached utilizing ring-shanked nails spaced on 6 in. (152 mm) centers.

Table 2.2 2x4 and 2x2 Specimen Configuration

Wall Size	1st Layer	2nd Layer	3rd Layer	4th Layer
2' x 4'	2x2 - H	2x2 - V	2x4 - SH	N/A
2' x 4'	2x2 - H	2x2 - V	2x4 - SH	2x4 - SH

2.3.3 Comprised of 1x2s

Two specimens that entirely consisted of 1x2s were constructed, one consisting of three layers and one of four layers (Table 2.3). Terms WV and WH refer to whether the 1x2s were loaded about the weak axis and either vertically or horizontally aligned, respectively (Figure 2.16).

Table 2.3 1x2 Specimen Configurations

Wall Size	1st Layer	2nd Layer	3rd Layer	4th Layer
4' x 4'	1x2 - WH	1x2 - WV	1x2 - WH	N/A
4' x 4'	1x2 - WV	1x2 - WH	1x2 - WV	1x2 - WH

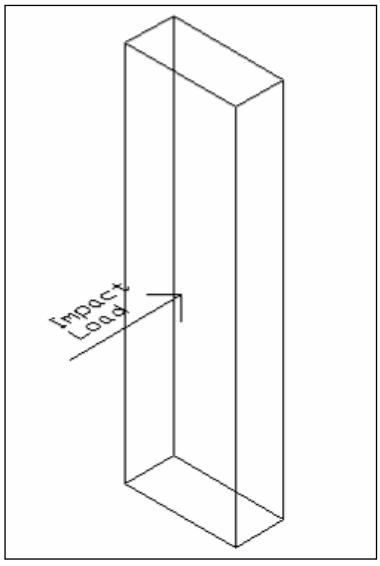

Figure 2.16 Weak Axis Bending

2.3.4 Comprised of 1x4s

A multitude of specimens solely comprised of 1x4s were constructed: two configurations consisting of three layers and multiple specimens four layers thick (Table 2.4).

Table 2.4 1x4 Specimen Configurations

Wall Size	1st Layer	2nd Layer	3rd Layer	4th Layer
4' x 4'	1x4 - WH	1x4 - WV	1x4 - WH	N/A
4' x 4'	1x4 - WV	1x4 - WH	1x4 - WV	N/A
4' x 4'	1x4 - WV	1x4 - WH	1x4 - WV	1x4 - WH

2.4 Fastener Configurations

2.4.1 Fastener Types and Characteristics

Three different types of fasteners were employed: screws, ring-shanked nails, and bolts. Size 6 screws (d = 0.161 in. [4.1 mm]) of varying lengths were used in all types of walls. 3 in. long ring-shanked nails (d = 0.135 in. [3.4 mm]) were used only in tests where the specimens were loaded so as to bend about the strong axis. Lastly, 1/2 in (12 mm) diameter all-thread bolts were used in conjunction with both screws and ring-shanked nails when testing 1 ft. (30 cm) by 1 ft. (30 cm) specimens.

Yield strength, σ_y, of each fastener was assumed as 50 ksi (344 MPa) for A527 steel. Table 2.5 provides the calculations for the shear, tensile yield, and withdrawal capacities of each fastener. Shear (F_τ) and the yield (F_σ) load capacities are expressed in kips, while the withdrawal (F_w) capacity measured in kips per inch (kN/mm).

Table 2.5 Loading Capacities of Fasteners

Type	σ_y (ksi)	D (in)	A (in^2)	F_τ (kips)	F_σ (kips)	F_w (k/in)
RS Nail	50	0.135	0.014	0.36	0.72	0.034
Screw	50	0.161	0.020	0.51	1.02	0.094
Bolt	50	0.5	0.196	4.91	9.82	N/A

2.4.2 Fastener Layouts

For bending about the strong axis, only one type of fastener layout was employed. Figure 2.17 illustrates this layout using 3 in. (76 mm) screws or 3 in. (76 mm) ring-shanked nails placed at 6 in. (152 mm) centers and staggered between the layers at 1/2 in. (12 mm) intervals.

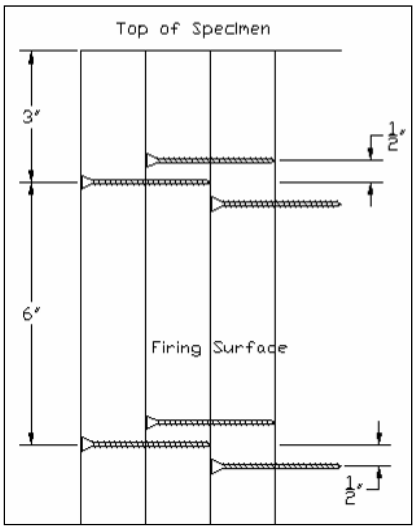

Figure 2.17 Front View of Strong Axis Fastener Distribution

One test on the weak axis included fasteners attached at every intersection of boards. As 13 boards comprise a single layer, 169 fasteners were utilized for each additional layer at 3.5 in. (89 mm) centers and is entitled "Every Intersection" (Figure 2.18). Because this and all specimens used weak axis tests, only screws were used as they possessed a much higher withdrawal capacity than ring-shanked nails.

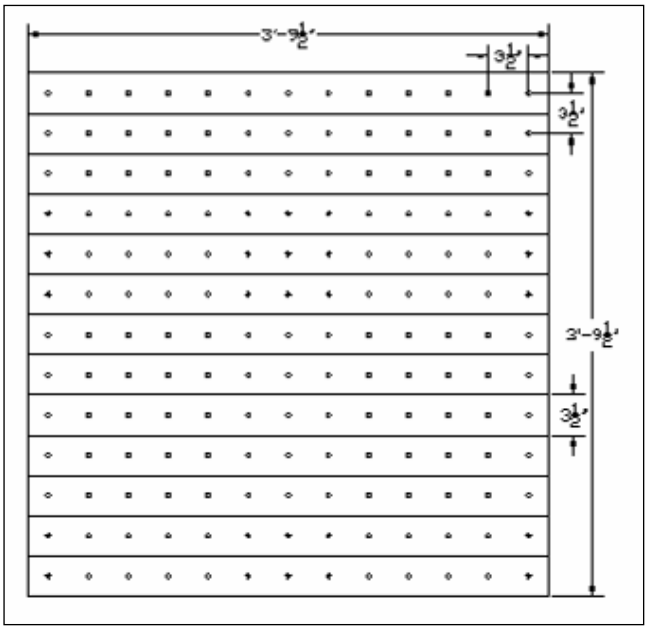

Figure 2.18 "Every Intersection" Fastener Distribution

The most common weak axis fastener layout is termed “Edge/Cross” because it employed fasteners placed at the edges of each specimen as well as vertically and horizontally through the centerlines of each axis of the specimen’s face (Figure 2.19).

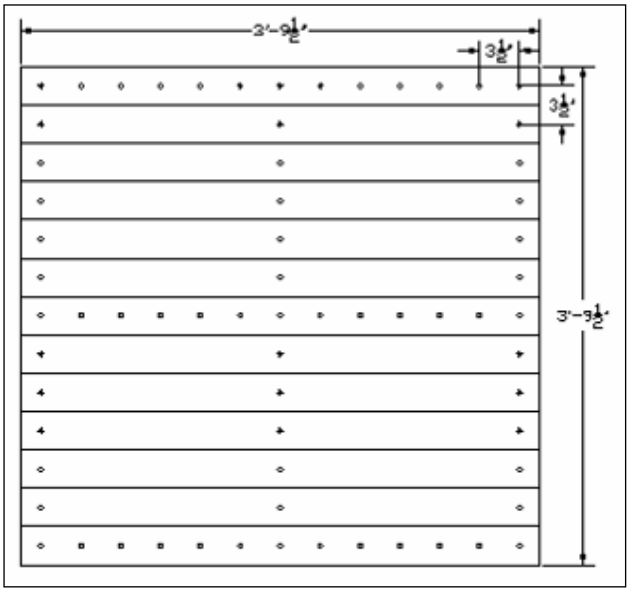

Figure 2.19 “Edge/Cross” Fastener Distribution

Figure 2.20 illustrates the “Edge/Star” fastener layout, another common weak axis layout, though this layout was not used as much as the “Edge/Cross” method. It is the same principle as the “Edge/Cross” but with additional fasteners added in an X pattern, forming a star pattern.

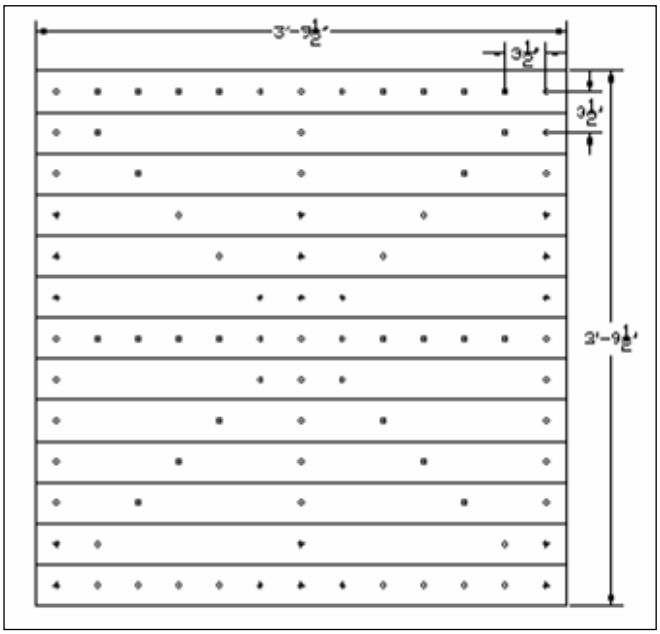

Figure 2.20 “Edge/Star” Fastener Distribution

2.4.3 Fastener Direction and Length

For tests on weak axis bending specimens, two different directional methods of installing fasteners were employed. Method 1 includes installing fasteners in opposite directions, with a single fastener only penetrating two boards at one time (Figure 2.21). Method 2 used fasteners of varying lengths that would penetrate every layer of the specimen but installed in only one direction (Figure 2.22).

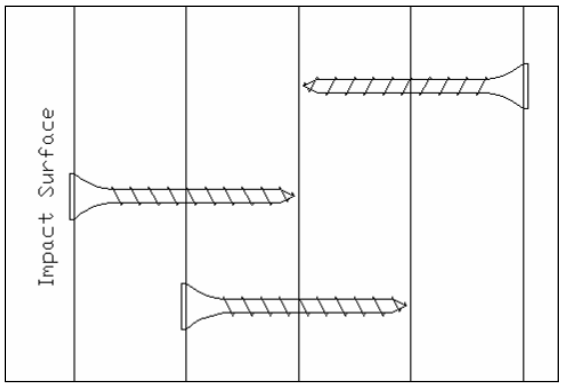

Figure 2.21 "Method 1" Fastener Directions

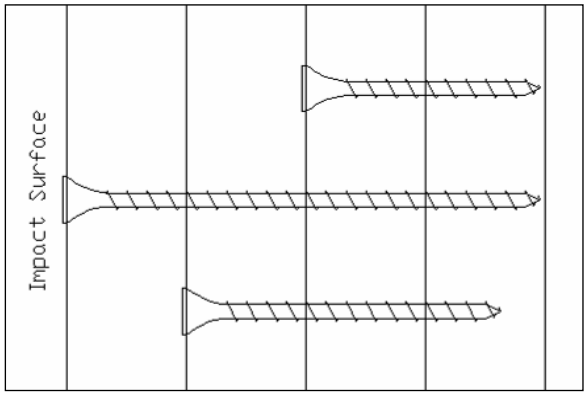

Figure 2.22 "Method 2" Fastener Directions

3. TEST RESULTS

3.1 Pass/Fail Impact Tests

3.1.1 Specimens Tested

Table 3.1 provides specimen configurations, the fasteners used, and if the specimen passed (no missile penetration and specimen did not display enough damage to negate a second test) or failed. Appendix B provides a more complete description of each test. "Test #" expresses the different tests performed throughout the research, while "Shot #" is the number of the impact test on each specific specimen. Most specimens failed on the first test so "Shot #" for most shots is only 1. "AOI" is the angle of impact. A 90° angle of impact represents an impact perpendicular to the face of the specimen, while a 0° angle of impact, though never used, would represent loading parallel to the face of the specimen. A specimen was considered as "passing" if the missile was stopped without significant damage to the wall. Test #s with a * represent specimens that were flexibly supported. SV, SH, WV, and WH refer to the orientation of the boards in the specimen: strong axis bending, vertically placed; strong axis bending, horizontally placed; weak axis bending, vertically placed; and weak axis bending, horizontally placed, respectively. "Centers" is the distance between fasteners or the method in which they were placed. M1 and M2 represent the way in which the fasteners were placed in the specimen: Method 1 (Figure 2.20) and Method 2 (Figure 2.21). Herein, all results will be provided in English units. Conversions are provided at the bottom of each page.

Table 3.1 Summary of Pass/Fail Impact Test Information

Test #	Wall Information							Fasteners			Veloc	Pass
	Wall Size	1st Layer	2nd Layer	3rd Layer	4th Layer	AOI	Shot #	Type	Length (in)	Centers (in)	mph	
1	4' x 8'	2x4 - SV	N/A	N/A	N/A	90	1	Screws	3	48	100	No
2	4' x 8'	2x4 - SV	2x4 - SH	N/A	N/A	90	1	Screws	3	6	100	No
3	2' x 4'	2x4 - SV	2x4 - SH	N/A	N/A	90	1	Screws	3	6	100	No
4	2' x 4'	2x4 - SV	2x4 - SH	N/A	N/A	90	2	Screws	3	6	100	No
5	2' x 4'	2x4 - SV	2x4 - SH	N/A	N/A	90	1	Screws	3	6	100	No
14	2' x 4'	2x4 - SV	2x4 - SH	N/A	N/A	90	1	Nails	3.25	6	100	No
15	2' x 4'	2x4 - SH	2x4 - SV	N/A	N/A	90	1	Screws	3.5	6	100	No
16	2' x 4'	2x4 - SV	2x4 - SH	N/A	N/A	90	2	Screws	3.5	6	100	No
17	2' x 4'	2x4 - SV	2x4 - SH	N/A	N/A	90	1	RS Nails	3.25	6	100	No
18	2' x 4'	2x2 - H	2x2 - V	2x4 - SH	N/A	90	1	RS Nails	3.25	6	100	No
19	2' x 4'	2x4 - SH	2x4 -SV	2x4 - SH	N/A	90	1	RS Nails	3.25	6	100	Yes
20	2' x 4'	2x4 - SH	2x4 -SV	2x4 - SH	N/A	90	2	RS Nails	3.25	6	100	No
21	2' x 4'	2x2 - H	2x2 - V	2x4 - SH	2x4 - SH	90	1	RS Nails	3.25	6	100	Yes
22	2' x 4'	2x2 - SH	2x2 - SV	2x4 - SH	2x4 - SH	90	2	RS Nails	3.25	6	100	No
23	4' x 4'	1x4 - WH	1x4 - WV	1x4 - WH	N/A	30	1	Screws	1.5	Each Int - M1	100	No
24	4' x 4'	1x4 - WH	1x4 - WV	1x4 - WH	N/A	45	2	Screws	1.5	Each Int - M1	100	No
25	1' x 1'	2x4 - SH	2x4 - SV	N/A	N/A	90	1	Screws	3.5	6"	100	No
26	1' x 1'	2x4 - SV	2x4 - SH	N/A	N/A	90	1	RS Nails	3.25	6"	100	No
27	4' x 4'	1x2 - WH	1x2 - WV	1x2 - WH	N/A	30	1	Screws	1.5	Edge/Cross - M1	100	Yes
28	4' x 4'	1x2 - WH	1x2 - WV	1x2 - WH	N/A	45	2	Screws	1.5	Edge/Cross - M1	100	No
29	4' x 4'	1x2 - WH	1x2 - WV	1x2 - WH	N/A	45	3	Screws	1.5	Edge/Cross - M1	100	No
30	4' x 4'	1x2 - WH	1x2 - WV	1x2 - WH	N/A	45	1	Screws	1.5	Edge/Cross - M1	100	No
31	4' x 4'	1x2 - WV	1x2 - WH	1x2 - WV	1x2 - WH	45	1	Screws	1.5	Edge/Cross - M1	100	No
32	4' x 4'	1x2 - WV	1x2 - WH	1x2 - WV	1x2 - WH	45	2	Screws	1.5	Edge/Cross - M1	100	No
33	4' x 4'	1x2 - WV	1x2 - WH	1x2 - WV	1x2 - WH	30	1	Screws	1.5	Edge/Cross - M1	100	Yes
34	4' x 4'	1x2 - WV	1x2 - WH	1x2 - WV	1x2 - WH	45	2	Screws	1.5	Edge/Cross - M1	100	No
35	4' x 4'	1x4 - WV	1x4 - WH	1x4 - WV	N/A	30	1	Screws	1.5	Edge/Cross - M1	100	Yes
36	4' x 4'	1x4 - WV	1x4 - WH	1x4 - WV	N/A	45	1	Screws	1.5	Edge/Star - M1	100	No
37	4' x 4'	1x4 - WV	1x4 - WH	1x4 - WV	1x4 - WH	45	1	Screws	1.5	Edge/Cross - M2	100	Yes
38	4' x 4'	1x4 - WV	1x4 - WH	1x4 - WV	1x4 - WH	45	1	Screws	Vary	Edge/Cross - M2	100	Yes
39	4' x 4'	1x4 - WV	1x4 - WH	1x4 - WV	1x4 - WH	45	1	Screws	Vary	Edge/Cross - M2	100	No
40	4' x 4'	1x4 - WV	1x4 - WH	1x4 - WV	1x4 - WH	45	1	Screws	Vary	Edge/Cross - M2	100	No
41	4' x 4'	1x4 - WV	1x4 - WH	1x4 - WV	1x4 - WH	45	1	Screws	Vary	Edge/Cross - M2	66.81	Yes
42*	4' x 4'	1x4 - WV	1x4 - WH	1x4 - WV	1x4 - WH	45	1	Screws	Vary	Edge/Cross - M2	63.25	Yes
43	4' x 4'	1x4 - WV	1x4 - WH	1x4 - WV	1x4 - WH	45	1	Screws	Vary	Edge/Cross - M2	75.67	Yes
44*	4' x 4'	1x4 - WV	1x4 - WH	1x4 - WV	1x4 - WH	45	1	Screws	Vary	Edge/Cross - M2	77.78	Yes
45	4' x 4'	1x4 - WV	1x4 - WH	1x4 - WV	1x4 - WH	45	1	Screws	Vary	Edge/Cross - M2	96	No
46*	4' x 4'	1x4 - WV	1x4 - WH	1x4 - WV	1x4 - WH	45	1	Screws	Vary	Edge/Cross - M2	103.82	Yes
47*	4' x 4'	1x4 - WV	1x4 - WH	1x4 - WV	1x4 - WH	45	1	Screws	Vary	Edge/Cross - M2	116.61	Yes
48	4' x 4'	1x4 - WV	1x4 - WH	1x4 - WV	1x4 - WH	45	1	Screws	Vary	Edge/Cross - M2	111.37	No
49*	4' x 4'	1x4 - WV	1x4 - WH	1x4 - WV	1x4 - WH	45	1	Screws	Vary	Edge/Cross - M2	111.28	Yes
50*	4' x 4'	1x4 - WV	1x4 - WH	1x4 - WV	1x4 - WH	90	1	Screws	Vary	Edge/Cross - M2	73.32	Yes
51*	4' x 4'	1x4 - WV	1x4 - WH	1x4 - WV	1x4 - WH	90	2	Screws	Vary	Edge/Cross - M2	83.22	Yes
52*	4' x 4'	1x4 - WV	1x4 - WH	1x4 - WV	1x4 - WH	90	3	Screws	Vary	Edge/Cross - M2	98.72	No
53*	4' x 4'	1x4 - WV	1x4 - WH	1x4 - WV	1x4 - WH	90	1	Screws	Vary	Edge/Cross - M2	101.10	No
54	4' x 4'	1x4 - WV	1x4 - WH	1x4 - WV	1x4 - WH	90	1	Screws	Vary	Edge/Cross - M2	82.50	Yes
55	4' x 4'	1x4 - WV	1x4 - WH	1x4 - WV	1x4 - WH	90	2	Screws	Vary	*Edge/Cross - M2*	80.01	No
56	4' x 4'	1x4 - WV	1x4 - WH	1x4 - WV	1x4 - WH	90	1	Screws	Vary	Edge/Cross - M2	106.80	No

3.1.2 Tests of Interest

It is not feasible to detail the results of all 56 tests listed in Table 3.1, so only selected and more pertinent test outcomes will be described. These were chosen either because of a passing (successful) result or, although no pass (unsuccessful) resulted, they provided results that could either be applied to later tests or gave other useful information.

One proposal for increasing the capacity of the specimen was to apply wood glue to the inside faces of the layers. Test #14 applied this idea but unfortunately showed no increase in load capacity of the specimen.[6]

Test #19 and #21 were the first specimens to pass a 90° impact test with bending about the components' strong axes (Figure 2.14). High speed video was taken of Test #19.[7] Test #19 consisted of three layers of 2x4s bending about the strong axis, with only approximately 0.5 in. (12 mm)[8] of deflection in the back layer while crushing the front layer around the impact zone. Test #21 consisted of two layers of 2x2s in front of two layers of 2x4s with the back layer only pushed out approximately 0.25 in. (6.4 mm) and both layers of 2x2s crushed around the impact zone. Figures 3.1a through 3.1e show five frames of the impact on Test #19. Figure 3.1a shows the moment of impact, while Figures 3.1b and 3.1c show the missile entering the specimen halfway and fully through the time of impact, respectively. Figures 3.1d and 3.1e show the missile exiting the specimen, breaking a section of a board with it. The high speed videos are located at the CSU Structures Lab website (CSU 2009).

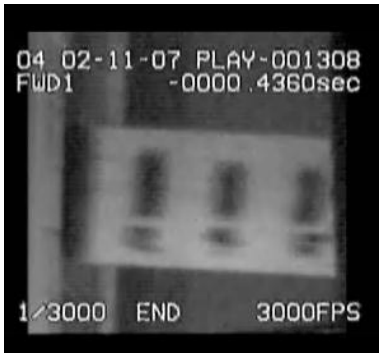

Figure 3.1a Test #19 (Impact)

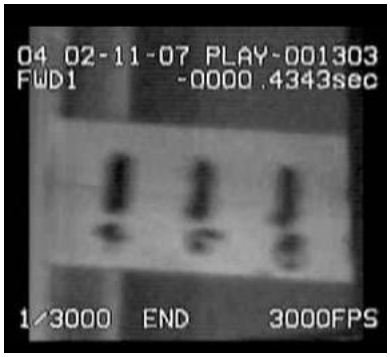

Figure 3.1b Impact+ .0017s

Figure 3.1c Impact+ .0033s

Figure 3.1d Impact+ 0.0053s

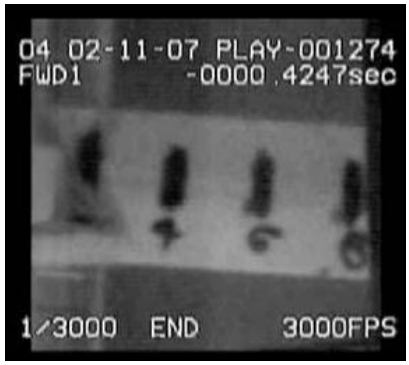

Figure 3.1e Impact+ 0.0113s

[6] No digitial photographs were taken of Shot #14.
[7] Neither digital video nor digital photographs were taken of Shot #21.
[8] 1 inch (in) = 2.54 centimeters (cm)

Although Tests #19 and #21 were successful, it was necessary to retest these specimens.[9] Tests #20 and #22 were the second tests of these specimens. Figures 3.2a through 3.2e are high speed camera stills at 0.0235 second intervals throughout the impact, pushing the rear layer back 5 in. (127 mm). Figures 3.2d and 3.2e show the missile being stopped by the specimen, though the specimen was significantly damaged. Being the second test on this specimen, more deformation was expected and the camera was zoomed farther out so as to capture 4 in. (102 mm) of deflection and/or deformation on the rear layer.[10]

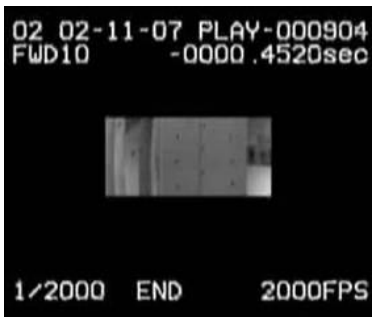

Figure 3.2a Test #20 (Impact)

Figure 3.2b Impact+ 0.0235sec

Figure 3.2c Impact + 0.0470s

Figure 3.2d Impact+0.0840s

Figure 3.2e Impact+0.0605s

[9] Because one of the project goals was to have a specimen that would survive multiple shots.
[10] Neither digital photographs nor regular speed video were taken of Shot #22.

One design idea was to build 1 ft. (30 cm) x 1 ft. (30 cm) specimens that would be adjoined to make a larger structure (Section 2.3.1). The idea of this structure was to minimize the unbraced length of the members under stress, which would aid in survival of the specimen. Tests #25 and #26 served to investigate this. Figures 3.3a and 3.3b give front and rear views of Test #26.[11] Specimens in Tests #25 and #26 were exactly alike with the exception of the fasteners utilized: screws and ring-shanked nails, respectively. These tests were considered failures because the specimen was significantly damaged and the rear layer was pushed out, even though the missile was stopped. Additional photographs are included at the CSU Structures Lab Web site (CSU 2009).

Figure 3.3a Front View of 1 ft. x1 ft. Impact (Test #26)

Figure 3.3b Rear View of 1 ft. x 1 ft. Impact (Test #26)

Tests #27 through #34 were all constructed using four crossing layers of 1x2s and the Edge/Cross fastener configuration and the Method 1 fastener direction. Tests #27 and #33 were fired at an impact angle of 30° with both specimens surviving with minimal damage. Since these tests easily withstood the load, Tests #28 and 32 were the second shot for each of these specimens and were fired at an impact angle of 45°. The missiles of both tests punctured the specimens with minimal damage to the missile. Figures 3.4a and 3.4b give post impact images for Tests #27 and #28, respectively.

Test #34 was different from Tests #28 and #32 in that while the missile punctured the specimen, it did not completely pass through the specimen, instead protruding approximately 3.5 ft. (1.1 m) after penetrating the specimen. Figures 3.5a and 3.5b show the post impact view of Test #34.

[11] No photographs were taken of Shot #25.

Figure 3.4a Test #27 Post Impact

Figure 3.4b Test #28 Post Impact

Figure 3.5a Test #34 Post Impact

Figure 3.5b Test #34 Post Impact (Close-up)

The specimens used for Tests #35 and #36 consisted of three layers of 1x4s connected using the Edge/Cross and Method 1 fastener configurations. Test #36 was the only test in which the specimen was fastened together using the Edge/Star distribution and also used the Method 1 fastener direction. The specimen for Test #37 was the first to survive a 45° angle of impact while bending about the weak axis (Figure 2.15). This specimen was the same configuration, and all subsequent specimens utilized the Edge/Cross and Method 2 fastener configurations. The major difficulty with this specific test is that a nut was accidentally not attached to the bolt at the front vertex of the base support. As a result, the specimen support structure rotated about the rear bolts and lifted up in the front directly after impact and then returned to its original position along with breaking approximately half the screws attaching the specimen to the support structure; even with this mistake, the test results were interesting as only the front layer was punctured with minimal damage on the rear layer. Figures 3.6a and 3.6b show the post-impact damage to the specimen, while Figure 3.6c is a video still at the moment the specimen support structure lifted up in the front. Regular speed video is included at the CSU Structures Lab Web site (CSU 2009).

Figure 3.6a Test #37 Post Impact Front View

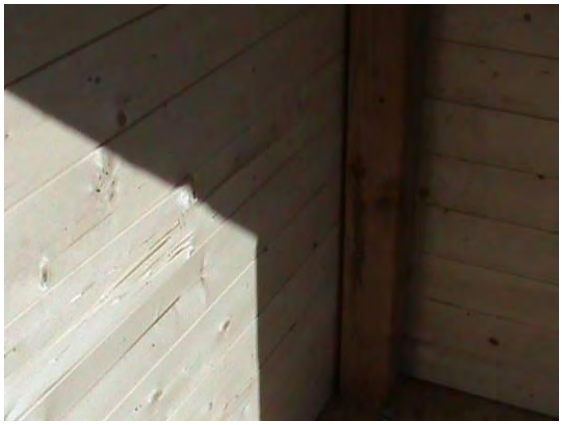

Figure 3.6b Test #37 Post Impact Rear View

Figure 3.6c Test #37 Video Still of Front Vertex Uplift

Test #38 also had an impact angle of 45°, with the key difference being that the both of the specimen walls separated from the base support while still stopping the missile. Figures 3.7a and 3.7b give front and rear views of the specimen after impact, while Figures 3.7c and 3.7d show the regular speed video impact still and post impact general view. In the figures, note that the missile impacted on the left specimen, though the right side is also damaged from a prior test.

Figure 3.7a Test #38 Impact Video Still

Figure 3.7b Test #38 Post-Impact General View

Figure 3.7c Test #38 Post Impact Rear View

Figure 3.7d Test #38 Post-Impact Front View

Figure 3.8a through 3.8f are high speed video stills from Test #39, in which the missile penetrated the specimen, but was stopped (similar to Test #33). Figure 3.8a shows the missile at the moment of impact with the specimen.

Figure 3.8a Test #39 (Impact)

Figure 3.8b Impact+ 0.024s

Figure 3.8c Impact+ 0.048s

Figure 3.8d Impact+ 0.071s

Figure 3.8e Impact+ 0.095s

Figure 3.8f Impact+ 0.123s

Since the distribution of the impact load was crucial toward the ability of the specimen to resist the test, the specimen used for Test #39 was disassembled layer by layer. Figures 3.8g through 3.8j show each layer, in which the boards that had a deflection of 0.25 in. (6.4 mm) or were severely damaged were turned on their side. This will be used for comparison to the statically loaded specimen layers shown in Section 3.2.2.

Figure 3.8g Test #39 Front Layer

Figure 3.8h Test #39 Second Layer

Figure 3.8i Test #39 Third Layer

Figure 3.8j Test #39 Rear Layer

Tests #41 through #49 were the second to last set of impact tests conducted in which high speed camera footage was taken. These tests were conducted at varying velocities at a 45° angle of impact with either rigid or flexible supports as indicated in Table 3.1. Figures 3.9a through 3.17c represent each of these successful tests, with three high speed camera stills for each test: a) at impact, b) at the moment of maximum local deflection, and c) at maximum global deflection. All tests stopped the missile, though Tests #45 and #48 were damaged too much to be considered successful tests (would obviously not pass a second test).

Figure 3.9a Test #41 Impact

Figure 3.9b Impact + 0.0023 sec

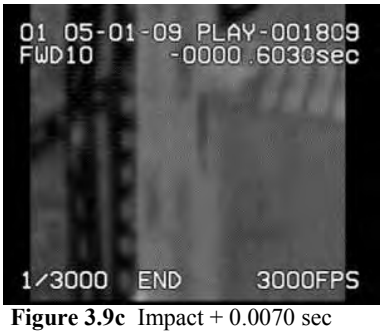

Figure 3.9c Impact + 0.0070 sec

Figure 3.10a Test #42 Impact

Figure 3.10b Impact + 0.0047 sec

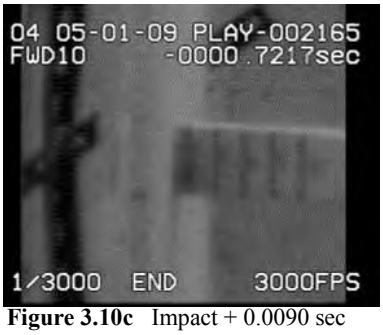

Figure 3.10c Impact + 0.0090 sec

Figure 3.11a Test #43 Impact

Figure 3.11b Impact + 0.0030 sec

Figure 3.11c Impact + 0.0140 sec

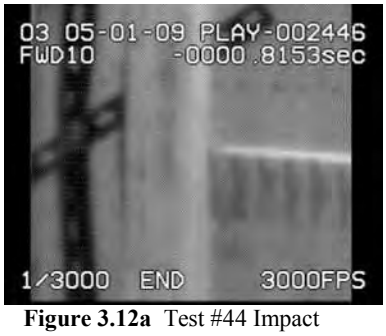

Figure 3.12a Test #44 Impact

Figure 3.12b Impact + 0.0070 sec

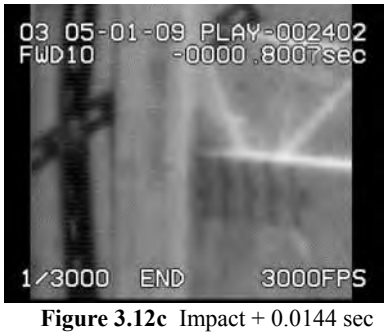

Figure 3.12c Impact + 0.0144 sec

Figure 3.13a Test #45 Impact

Figure 3.13b Impact + 0.0036 sec

Figure 3.13c Impact + 0.0096 sec

Figure 3.14a Test #46 Impact

Figure 3.14b Impact + 0.0050 sec

Figure 3.14c Impact + 0.0093 sec

Figure 3.15a Test #47 Impact

Figure 3.15b Impact + 0.0047 sec

Figure 3.15c Impact + 0.0147 sec

Figure 3.16a Test #48 Impact

Figure 3.16b Impact + 0.0063 sec

Figure 3.16c Impact + 0.0096 sec

Figure 3.17a Test #49 Impact

Figure 3.17b Impact + 0.0023 sec

Figure 3.17c Impact + 0.0040 sec

Tests #50 through #56 were the last set of impact tests conducted in which high speed camera footage was taken. These tests were conducted at varying velocities with a 90° angle of impact with either rigid or flexible supports as indicated in Table 3.1. Figures 3.18a through 3.24c represent each of these successful tests, with three high speed camera stills for each test: a) at impact, b) at the moment of maximum local deflection, and c) at maximum global deflection (successful tests) or post-penetration (failed tests). Tests #50, #51, and #54 successfully stopped the missile without significant damage, while Tests #52 and #53 were failures that still stopped the missile (Figures 3.20d, 3.21d, and 3.23d).

Figure 3.18a Test #50 Impact (Pass)

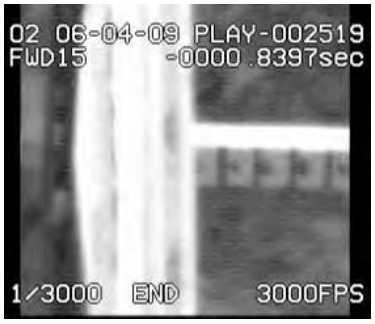

Figure 3.18b Impact + 0.0043 sec

Figure 3.18c Impact + 0.0100 sec

Figure 3.19a Test #51 Impact (Pass)

Figure 3.19b Impact + 0.0053 sec

Figure 3.19c Impact + 0.0154 sec

Figure 3.20a Test #52 Impact (Fail)

Figure 3.20b Impact + 0.0040 sec

Figure 3.20c Impact + 0.0087 sec

Figure 3.20d Test #52 Post Impact

Figure 3.21a Test #53 Impact (Fail)

Figure 3.21b Impact + 0.0043 sec

Figure 3.21c Impact + 0.0150 sec

Figure 3.21d Test #53 Post Impact

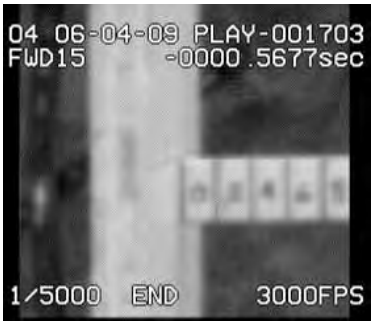

Figure 3.22a Test #54 Impact (Pass)

Figure 3.22b Impact + 0.0044 sec

Figure 3.22c Impact + 0.0104 sec

Figure 3.23a Test #55 Impact (Fail)

Figure 3.23b Impact + 0.0044 sec

Figure 3.23c Impact + 0.0170 sec

Figure 3.23d Test #55 Post Impact

Figure 3.24a Test #56 Impact (Fail)

Figure 3.24b Impact + 0.0037 sec

Figure 3.24c Impact + 0.0077 sec

3.1.3 Load, Energy, Deflection

From the high speed video capture of Test #19, the duration of impact (T_{Impact}) was measured as 3.4 milliseconds. This was the time difference in the high speed video from the moment of impact to the moment that the missile began to travel backward from its original direction. Using Equation 1.2, the load on the specimen was calculated as 17.6 kips (78 kN) as shown in Table 3.2, corresponding to an impact pressure of 3.37 ksi (23 MPa). Additionally, the table provides the calculated kinetic energy at impact (KE_{Impact}) to be resisted by the specimens during each test. For a detailed computation, refer to Appendix C. This is important for comparison between a more rigid specimen (Test #19) and later tests utilizing more flexible specimens.

Table 3.2 90° Successful Rigid Specimen Support: Force Calculations

Test #	T_{Impact} (sec)	V_{avg} (ft/sec)	V_{avg} (mph)	m (slugs)	F_{Impact} (kips)	p_{Impact} (ksi)	KE_{Impact} (ft-lbs)
19	0.0034	176	**120**	0.34	**17.6**	3.35	**5266**

Tables 3.3 and 3.4 provide the calculations based on Equation 1.2 to determine both the resultant and vector components of the forces (F_{impact}) representing successful specimens loaded at a 45° angle of attack. Table 3.3 includes specimens with rigid supports, while Table 3.4 includes specimens with flexible supports. Additionally, Tables 3.3 and 3.4 provide the times of impact and local deflections of the specimens with passing tests along with missile impact velocities as determined through the high speed camera footage.

Table 3.3 45° Successful Rigid Support: Force Calculations

Test #	T_{impact} (sec)	Δ (in)	V_{avg} (ft/sec)	V_{avg} (mph)	m (slugs)	F_{Impact} (kips)	p_{Impact} (ksi)	$F_{45°}$ (kips)	KE_{Impact} (ft-lbs)
41	0.0047	0.783	97.98	**66.81**	0.34	**7.12**	1.36	**5.04**	**1640**
43	0.0027	0.782	110.99	**75.67**	0.34	**14.04**	2.67	**9.93**	**2104**

Table 3.4 45° Successful Flexible Support: Force Calculations

Test #	T_{impact} (sec)	Δ (in)	V_{avg} (ft/sec)	V_{avg} (mph)	m (slugs)	F_{Impact} (kips)	p_{Impact} (ksi)	$F_{45°}$ (kips)	KE_{Impact} (ft-lbs)
42	0.007	0.346	92.76	**63.25**	0.34	**4.53**	0.86	**3.20**	**1470**
44	0.003	0.589	114.07	**77.78**	0.34	**12.99**	2.47	**9.19**	**2223**
46	0.0037	0.947	152.28	**103.82**	0.34	**14.06**	2.68	**9.94**	**3961**
47	0.0033	0.601	171.03	**116.61**	0.34	**17.71**	3.37	**12.52**	**4996**
49	0.0029	0.399	163.21	**111.28**	0.34	**19.23**	3.66	**13.59**	**4550**

Table 3.5 provides the calculations for Tests #50, #51, and #54 to determine the overall load on the specimen at a 90° angle of impact. Tests #50 and #51 were flexibly supported while Test #54 was rigidly supported. These calculations were performed using Equation 1.2 and an expanded view is shown in Appendix C.

Table 3.5 90° Successful Tests: Force Calculations

Test #	T_{impact} (sec)	V_{avg} (ft/sec)	V_{avg} (mph)	m (slugs)	F_{Impact} (kips)	p_{Impact} (ksi)	KE_{Impact} (ft-lbs)
50	0.008	107.54	**73.32**	0.34	**4.59**	0.87	**1975**
51	0.0067	122.06	**83.22**	0.34	**6.22**	1.19	**2545**
54	0.006	121.00	**82.50**	0.34	**6.89**	1.31	**2501**

There are three observations that are important to note from these tables. First, the flexible specimens (Tables 3.3, 3.4, and 3.5) had significantly lower overall loads than the more rigid specimen (Table 3.2) Second, there were significantly more flexibly supported specimens surviving 45° tests and at higher velocities (Tables 3.3 and 3.4). Third, the duration of impact (T_{impact}) ranged between 2.7 ms and 8 ms, while the impact force (F_{impact}) ranged from 3.2 kips (14 kN) to 17.6 kips (78 kN). Last, combined with knowledge of the overall damage to the specimens after testing, flexibly supported specimens resisted the impact loads at 90° better than the rigidly supported specimens, though the overall impact forces were similar in magnitude.

3.2 Static Load Tests

3.2.1 Specimens Tested

Three static load tests were completed, which were composed of four layers of 1x4s bending about the weak axis with screws installed using Method 2 in the manner of specimens for Tests #37 through 56, as described in Section 3.1.1. Deflection measurements were taken at 0.25 kip (1.1 kN) load intervals.

3.2.2 Load vs. Deflection

3.2.2.1 Static Test #1

At the 5.60 kip (25 kN) load level, the specimen began to progressively crack (quick drop in load at same deflection also evident from cracking sounds) as the load was increasing. Figure 3.25 is an illustration of the load versus centerpoint deflection for the specimen. At the 5.48 kip (24 kN) load level, the specimens reached an apparent elastic limit. At 7.15 kips (32 kN), the specimen failed (increased in deflection without a load increase) and the test was terminated. The area under the load-deflection curve, which is also provided in Figure 3.25, constitutes the energy stored in the specimen during loading. The energy stored at the elastic limit was 364 ft.-lb. (494 J) while the energy stored at failure was 1422 ft.-lb. (1928 J).

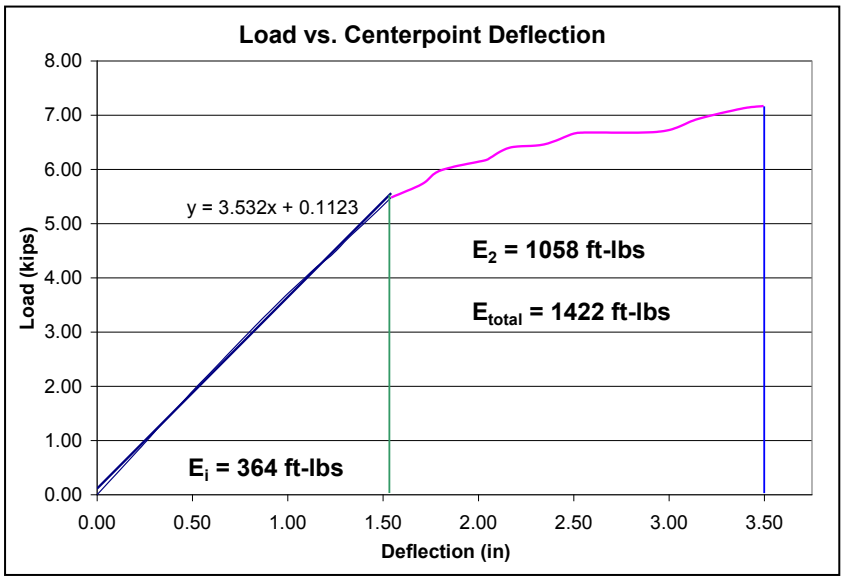

Figure 3.25 Static Test #1 Load vs. Centerpoint Deflection

Table 3.6 provides the deflections for loads at approximately 1.0 kip (4.45 kN) intervals, as well as the deflections at the 5.48 kip (24 kN) and 7.15 kip (32 kN) load levels. Figures 3.26 and 3.27 give an illustration of the deflections along the X and Y axes, respectively. End deflections were assumed as 0.00 at both edges along the Y axis and at one edge of the X axis as they were supported, while the deflection of the unsupported (west) edge was not measured, thus is not included in Figure 3.26. The upper and lower bold lines in these figures are the deflected shapes of the specimen at the 5.48 kip (24 kN) and 7.15 kip (32 kN) load levels.

Table 3.6 Static Test #1 Load vs. Deflection

Load (kips)			0.99			2.00			2.99			3.98		
Δ (in)	SW	West	NW	0.152	0.233	0.205	0.292	0.467	0.389	0.435	0.707	0.571	0.590	0.963	0.756
	S	Cen	N	0.159	0.259	0.206	0.308	0.524	0.388	0.463	0.796	0.570	0.617	1.084	0.759
	SE	East	NE	0.133	0.148	0.128	0.224	0.293	0.239	0.276	0.441	0.354	0.364	0.592	0.467

4.98			**5.48**			5.98			6.93			**7.15**		
0.755	1.241	0.956	0.842	**1.372**	1.058	0.923	1.503	1.165	1.290	2.199	1.654	1.411	**2.460**	1.826
0.776	1.394	0.951	**0.851**	**1.543**	**1.039**	0.940	1.803	1.146	1.320	3.152	1.640	**1.422**	**3.536**	**1.787**
0.510	0.746	0.586	0.570	**0.822**	0.642	0.561	0.901	0.712	0.751	1.331	1.053	0.849	**1.453**	1.147

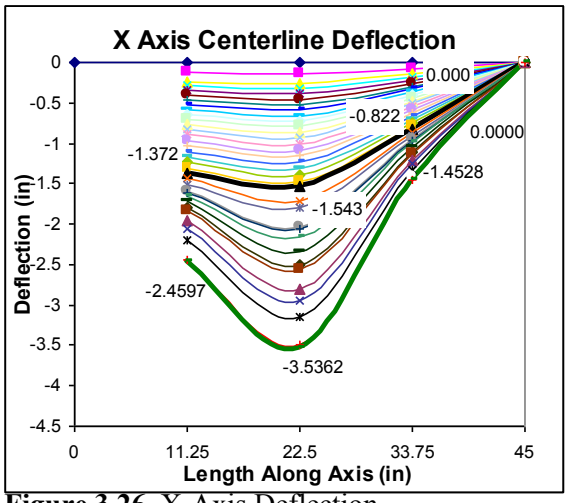

Figure 3.26 X-Axis Deflection

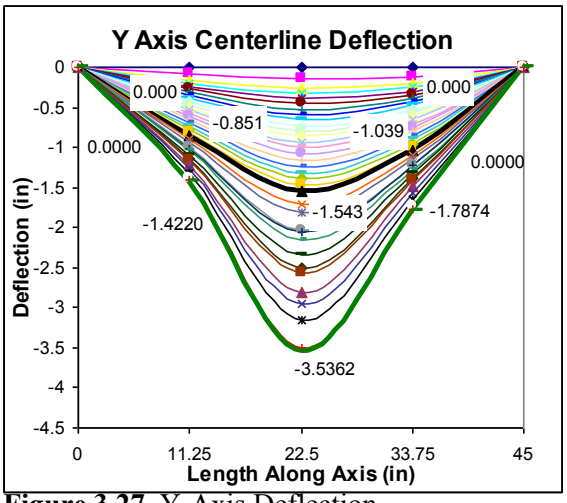

Figure 3.27 Y-Axis Deflection

Since a possible key factor in specimen survival is the ability to distribute the load throughout the various layers, the failed specimen was taken apart layer by layer. Figures 3.28 through 3.31 show each layer after removal from the overall specimen. The boards that are turned on their sides are boards in which the deflection at either end, when laid flat, was greater than 0.25 in. (6.4 mm), giving a general representation as to how the load was spread throughout the specimen. This is also in comparison with Figures 3.8g through 3.8j to show how a statically loaded specimen in which the duration of loading is significantly longer spreads the load between the various layers, thus providing a significantly different response than in the impact loading tests.

Figure 3.28a Static Load 1 Front Layer

Figure 3.28b Static Load 1 Second Layer

Figure 3.28c Static Load 1 Third Layer

Figure 3.28d Static Load 1 Rear Layer

3.2.2.2 Static Test #2

In Static Test #2, load was applied to the specimen only until it cracked for the first time. As such, this test was stopped at the initial cracking, occurring at the 6.77 kip (30 kN) load level. However, the final deflection reading had been taken at 6.46 kips (28.7 kN), which resulted in a centerpoint deflection of 1.96 in. (50 mm), as shown in Figure 3.29. The energy stored in the specimen at the elastic limit was calculated as 529 ft.-lb. (717 J) (Equation 1.3). Table 3.7 provides selected load vs. adjusted deflection values for the second test at approximately 1.0 kip (4.5 kN) intervals with the results at 6.46 kips (28.7 kN), also provided. Figure 3.30 and 3.31 provide the centerline deflections for this test, with the previously mentioned end conditions still applicable.

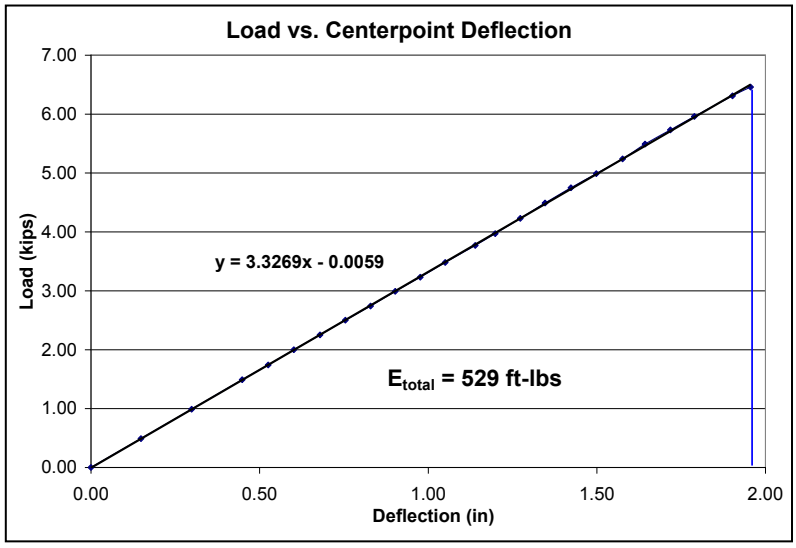

Figure 3.29 Static Test #2 Load vs. Centerpoint Deflection

Table 3.7 Static Test #2 Load vs. Deflection

Load (kips)			0.99			2.00			2.99			3.97		
Δ (in)	SW	West	NW	0.152	0.234	0.162	0.331	0.492	0.327	0.508	0.749	0.490	0.688	1.010	0.648
	S	Cen	N	0.181	0.299	0.215	0.370	0.602	0.405	0.557	0.902	0.580	0.741	1.199	0.752
	SE	East	NE	0.141	0.209	0.176	0.255	0.385	0.312	0.371	0.552	0.438	0.484	0.713	0.561

4.99			5.96			**6.46**		
0.876	1.277	0.814	1.062	1.536	0.971	1.165	**1.685**	1.063
0.926	1.499	0.919	1.099	1.789	1.077	**1.188**	**1.956**	**1.162**
0.597	0.874	0.679	0.706	1.027	0.790	0.762	**1.113**	0.843

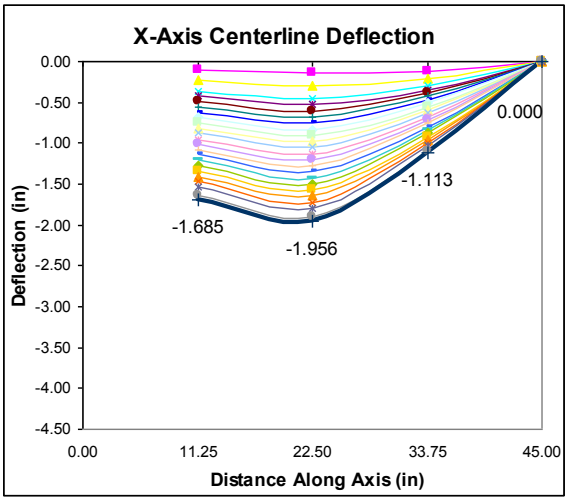

Figure 3.30 X-Axis Deflection

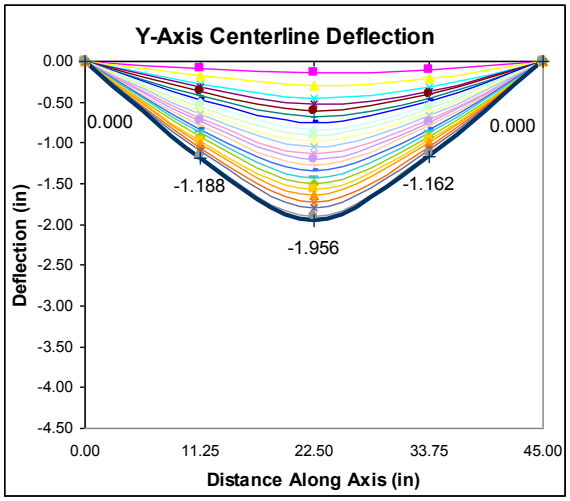

Figure 3.31 Y-Axis Deflection

3.2.2.3 Static Test #3

The specimen in Test #3 was loaded to failure. It was conceived that errors could have occurred in the first two tests at low load levels due to gaps between the boards. Mortar was placed along the supported edges for Test #3 to provide for desired consistent support conditions. The load did not increase after multiple cracks began occurring and the deflection continued to increase, reaching a plateau at the 6.58 kip (30 kN) load level. The final reading before failure was taken at 6.46 kips (29 kN), which resulted in a centerpoint deflection of 2.11 in. (54 mm), as shown in Figure 3.32. The specimen resisted linearly up until a load of 5.98 kips (27 kN), corresponding to a deflection of 1.68 in. (43 mm). The energy stored in the specimen at the elastic limit was calculated as 468 ft-lbs (635 J) while the energy stored at failure was 660 ft.-lb. (895 J). Table 3.8 provides load vs. adjusted deflection values for the specimen at approximately 1.0 kip (4.5 kN) intervals up to 6.00 kips (27 kN), and the results at 6.20 kips (28 kN) and 6.46 kips (29 kN) also provided. Figure 3.33 and 3.34 provide the centerline deflections for this test, with the previously mentioned end conditions still applicable.

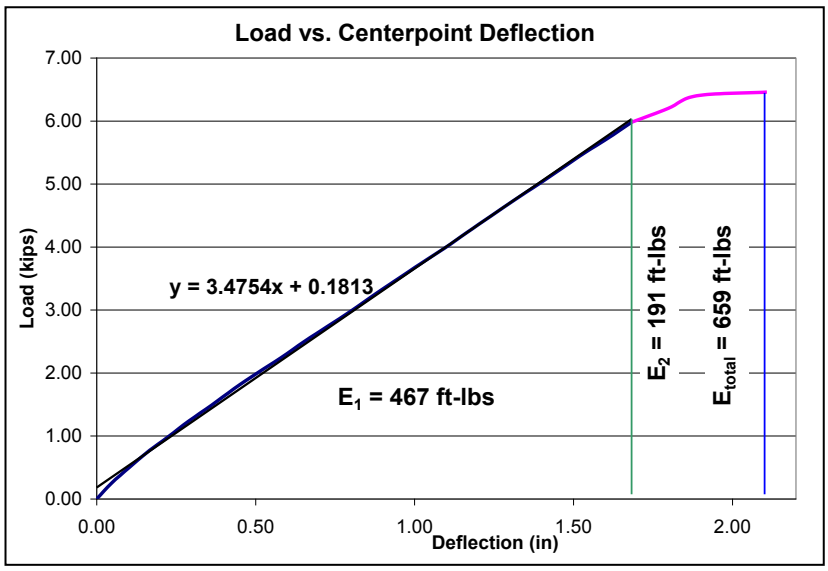

Figure 3.32 Static Test #3 Load vs. Centerpoint Deflection

Table 3.8 Static Test #3 Load vs. Deflection

	Load (kips)			0.99			2.00			2.99			3.98		
Δ (in)	SW	West	NW	0.140	0.179	0.150	0.304	0.422	0.322	0.479	0.695	0.506	0.650	0.961	0.684
	S	Cen	N	0.148	0.226	0.161	0.316	0.506	0.334	0.493	0.802	0.517	0.659	1.094	0.700
	SE	East	NE	0.107	0.140	0.140	0.229	0.300	0.228	0.346	0.464	0.347	0.459	0.624	0.448

5.00			**5.98**			6.20			**6.46**		
0.820	1.227	0.864	0.989	**1.494**	1.044	1.041	1.583	1.104	1.146	**1.774**	1.230
0.821	1.391	0.880	**0.975**	**1.683**	**1.050**	1.018	1.798	1.105	**1.102**	**2.109**	**1.217**
0.571	0.779	0.533	0.673	**0.928**	0.649	0.703	0.978	0.680	0.755	**1.086**	0.748

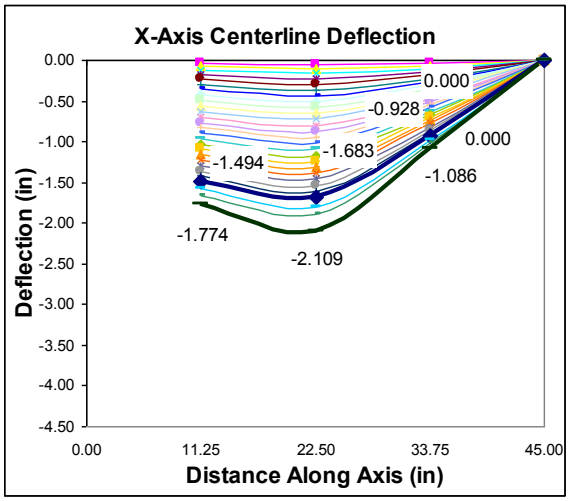

Figure 3.33 X-Axis Deflection

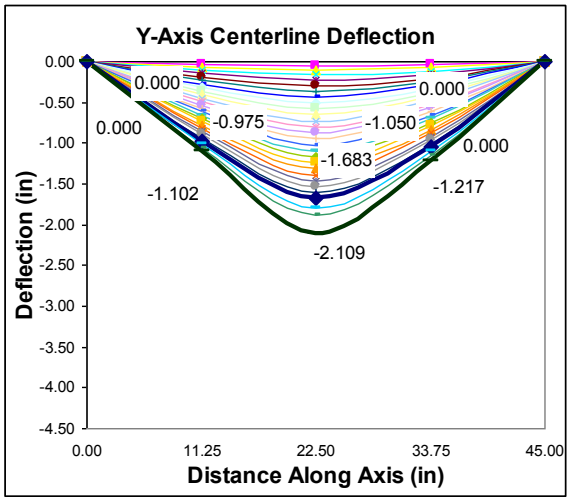

Figure 3.34 Y-Axis Deflection

4. DISCUSSION

The research described herein had the goals of (a) design an all wood wall "specimen" that could withstand impact loads set forth by FEMA 361 specifications, (b) observe how key components (specimen geometry, fastener type and arrangement, loading variations, and support configurations) affect the behavior of the specimen under impact loading, and (c) observe how materials perform under very short duration, high impact loadings.

As tests were conducted it became apparent that the design characteristics of the system that supported the wall specimen were as important as the design characteristics of the wall specimen itself, both of which are discussed in the following sections.

4.1 Specimen Configurations

Sixteen different wall specimen configurations, as described earlier in Table 3.1, were tested under impact loading. Only three of these configurations were reasonably successful, meaning that they prevented penetration by 2x4 missiles at velocities at or near FEMA standards. These configurations were: (A) 2 layers 2x2 + 2 layers 2x4 (strong axis), (B) 3 layers 2x4 (strong axis), and (C) 4 layers 1x4 (weak axis) as shown in Table 3.1. The layers for each specimen were orthogonally aligned to each adjacent layer.

Tests on specimen configurations A and B showed that these designs needed to be solid and significantly thicker (i.e., 10.5 in. [267 mm]) for tornado protection (i.e., prevent penetration of a single impact at 100 mph [161 km/h]) than stud walls commonly used in construction. Although they survived an initial impact test, additional impact tests on these specimens resulted in wall penetration failure, meaning that they would not survive repeated impact tests. Interestingly, specimen A had about half the maximum deflection and performed far better than specimen B for tornado protection requirements.

Tests on the thinner (3.0 in. [76 mm]) and more flexible specimen C showed that lighter weight, more flexible designs could be more successful as compared with A and B. Though the lighter weight designs were not able to resist a 100 mph (161 km/h), 90° angle of impact test, they did show promise with resisting multiple tests at slightly slower velocities. Four layers of 1x4 boards were required to survive the test loadings.

4.2 Fastener Configurations

Impact load tests on specimens with elements bending about the strong axis (types A and B) demonstrated that the variation of fasteners (i.e., screws, nails. ring-shanked nails) did not substantially affect specimen strength.

For specimen C configuration, variation in fastener configuration had the potential to affect test results. Fasteners that were installed in a single direction (Method 2) proved to be more effective than fasteners installed in both directions (Method 1), with specimens using Method 2 being more likely to survive impact tests by apparently tightening the system together.

Because fasteners needed to resist forces along the longitudinal axis (as opposed to shear forces), only screws were used in these tests. Lastly, increasing the number of fasteners beyond the "Edge/Cross" method did not significantly affect specimen strength or improve test results.

Overall for these specimens, while the Edge/Star and Every Intersection connection methods provided similar results to Edge/Cross specimens, these configurations required more fasteners and a significantly

greater amount of work without yielding better results. Method 1 called for fasteners of equal lengths inserted between two layers set in different directions (Figure 2.21). When Method 2 (Figure 2.22) was employed, the specimens showed a significant increase in resistance. This is attributed to the fact that not only were the fasteners in the same direction, but were of different lengths so any load transferred to the final layer would be transferred back to the other layers, creating more of a basket load distribution scenario.

4.3 Loading Variations

4.3.1 Angle of Impact

As expected, the angle of impact had a significant effect on the ability of the specimen to resist the impact load. Specimen configurations A and B were the only ones to survive a single 90° impact angle test above 100 mph (161 km/h), though they failed a second impact test and were penetrated by the missile.

For configuration C, many tests with 30° and 45° angles of impact were successful. All specimens tested at 30° passed at the velocities tested, typically around 100 mph (161 km/h). These were supported by the two wall support structures. Specimens tested at 45° were able to withstand the load at velocities near or above 100 mph (161 km/h) only if they used flexible support systems. When a 90° angle of impact was tested, both flexibly and rigidly supported specimens were able to withstand a test velocity of around 83 mph (134 km/h) vs. 82 mph (132 km/h) of Texas Tech, though tests on flexibly supported specimens suggested that they may be able to resist test velocities in the 90-95 mph (145-153 km/h) range.

In summary, the specimen was progressively more likely to resist the impact load the farther from a 90° angle of impact the missile struck the specimen because these angles resulted in a transfer of less load perpendicular to the specimen face. All specimens survived all shots with a 30° angle of impact. While the thin-walled specimens with a 45° angle of impact did not necessarily survive, some passed the tornado magnitude test (with the support conditions playing a large role). After completing tests with a 90° angle of impact on thin walled specimens, it is estimated that the threshold of the specimens at this angle is in the range of 90-95 mph (145-153 km/h). While the decrease in load capability at the change of the angle is expected, it is an important observation for future research into complete structures.

4.3.2 Test Velocity

Different velocities were used in tests conducted near the end of the study at 45° and 90° angles of impact on the thinner, more flexible specimens (Table 3.1, Tests #38 - #56). Velocities of approximately 65, 75, 100, and 115 mph (105, 121, 161, and 185 km/h) were tested with specimens at 45° angles of impact using both rigid and flexible support conditions. At lower velocities of 65 mph (105 km/h) and 75 mph (121 km/h), both rigid and flexibly supported specimens resisted penetration. At higher velocities of 100 mph (161 km/h) and 115 mph (185 km/h), only flexibly supported specimens were successful, with one surviving a 103 mph (166 km/h) velocity for the first shot and a subsequent shot at 116 mph (187 km/h). This suggests that these specimens could withstand missile impacts at tornado velocity levels at a 45° impact angle, but also may be able to withstand missile impacts at tornado velocity levels while surviving multiple loadings.

For the specimens with a 90° angle of impact, the velocities used for testing were around 73, 80, 83, and 100 mph (118, 129, 134, and 161 km/h) with specimens utilizing either rigid or flexible supports surviving the 83 mph (134 km/h) range firings. Interestingly, the flexibly supported specimen was able to withstand this loading after a previous firing at 73 mph (118 km/h), while the rigidly supported specimen had cracking of the rear layer after a single shot at 82.5 mph (133 km/h). Another remarkable result of

the testing showed that the flexibly supported specimen failed the test but stopped the missile at about 100 mph (161 km/h) (Figures 3.20d and 3.21d) with Shot #53 only allowing approximately 14 in. (36 cm) of penetration. This suggests that the envelope for success at a 90° angle of impact is in the 90-95 mph (145-153 km/h) velocity range.

4.3.3 Impact vs. Static

Impact tests also provided useful and significant information to understand how the specimens responded under very short duration loads. First, the loads resisted during 90° impact tests were not considerably larger than the loads at the elastic limit during static loading when comparing the loads resisted in the impact tests in Table 3.5 and the static tests in Tables 3.6-8. There are two reasons that this occurs. First, the impulse momentum relationship assumes a constant load on the specimen, but this is unlikely to be the case. In reality, the force on the specimen under impact loading is spiked, while the static load plateaus. Figure 4.1 illustrates the fact that the average value for the impact load and the static load may be similar, but the actual maximum loads may be drastically different. The maximum values were not able to be calculated.

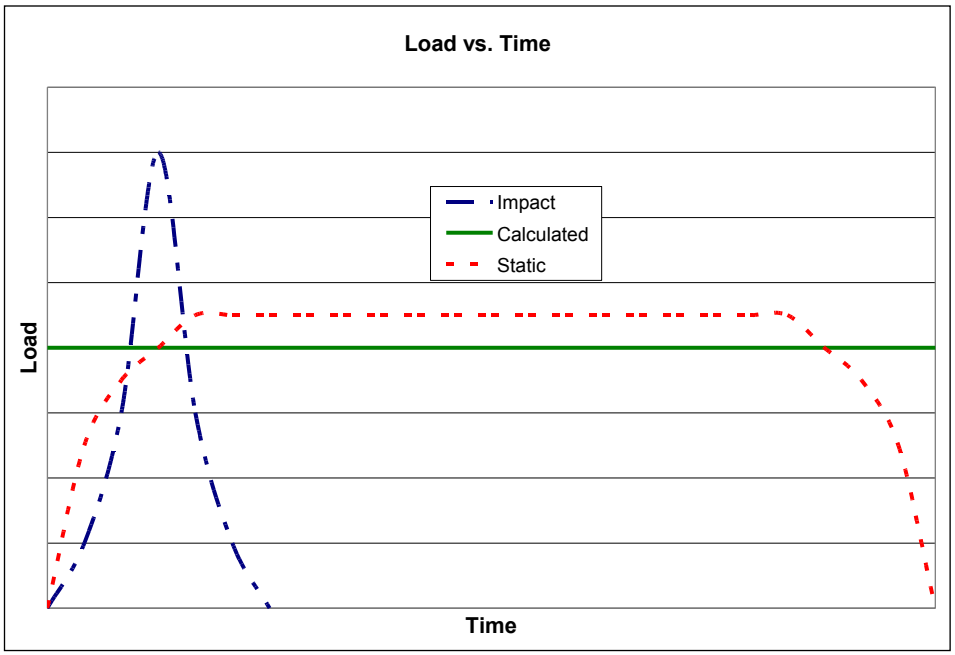

Figure 4.1 Load vs. Time for Impact, Static, and Calculated Loadings

This is more likely to do with the flexible supports absorbing energy and energy being transferred back to the missile (causing it to bounce off the specimen) than rejecting the conclusions of ultimate strength increase of Elmendorf, Liska, and Wood. It is interesting to see that, despite the difference in response in the static testing, the load at failure was similar and it would be interesting to do future studies to model the stress distributions and deflection patterns in the impact tests compared with the static load tests. Such an impact load model would necessitate incorporating physical knowledge of wood properties under extremely rapid impact loading. Figures 4.2 (Energy vs. Velocity) and 5.3 (Energy vs. Load Duration) show that the energy absorbed during the impact tests is 3.7 to 7.0 times that of the energy stored during static loading. The durations of load for Figure 4.3 were determined from high speed video for the impact tests and were calculated as the deflection (inches) (mm) divided by the loading rate (inches/sec) (mm/sec). These figures also provide the impact energies for 90, 92.5, and 95 mph (145, 149, and 153

km/h) impact velocities that were estimated, not tested, to be in the range of maximum allowable test velocities for flexibly supported specimens. In addition, the nature of the tests provided useful insight as to how composite specimens - designed to act like netting - distributed loads throughout the specimen. It was also of interest to compare the energy absorbed by the specimens at failure. Figure 4.4 compares the energy stored in the specimen at ultimate failure in Static Tests #1 and #3 (Test #2 was not loaded to failure) to the kinetic impact energy for Tests #52 and #53, which failed the impact test but only allowed a small amount of penetration. Figure 4.4 also includes the kinetic impact energies for 90, 92.5, and 95 mph (145, 149, and 153 km/h), which were estimated to be the threshold velocities for success for this specimen configuration. The important observation from this chart is the impact tests withstanding 2.5 to 5.7 times the amount of kinetic impact energy over the energy absorbed by the statically loaded specimens.

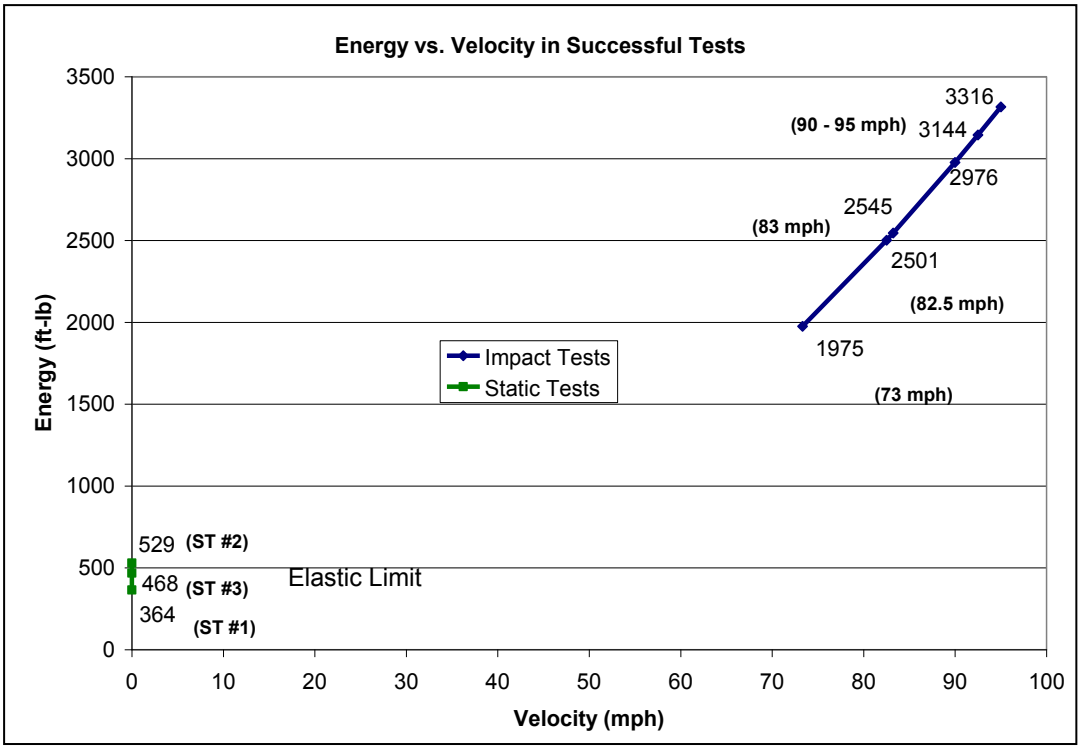

Figure 4.2 Energy vs. Velocity for Passing Specimens

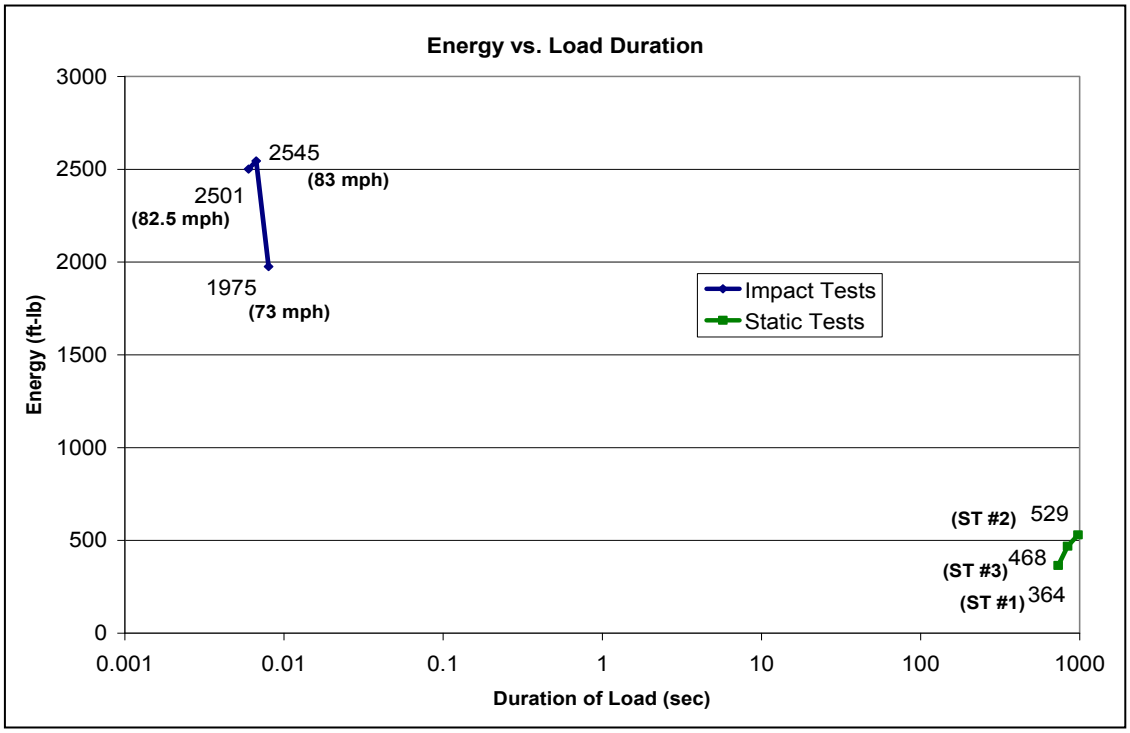

Figure 4.3 Energy vs. Load Duration for Passing Specimens

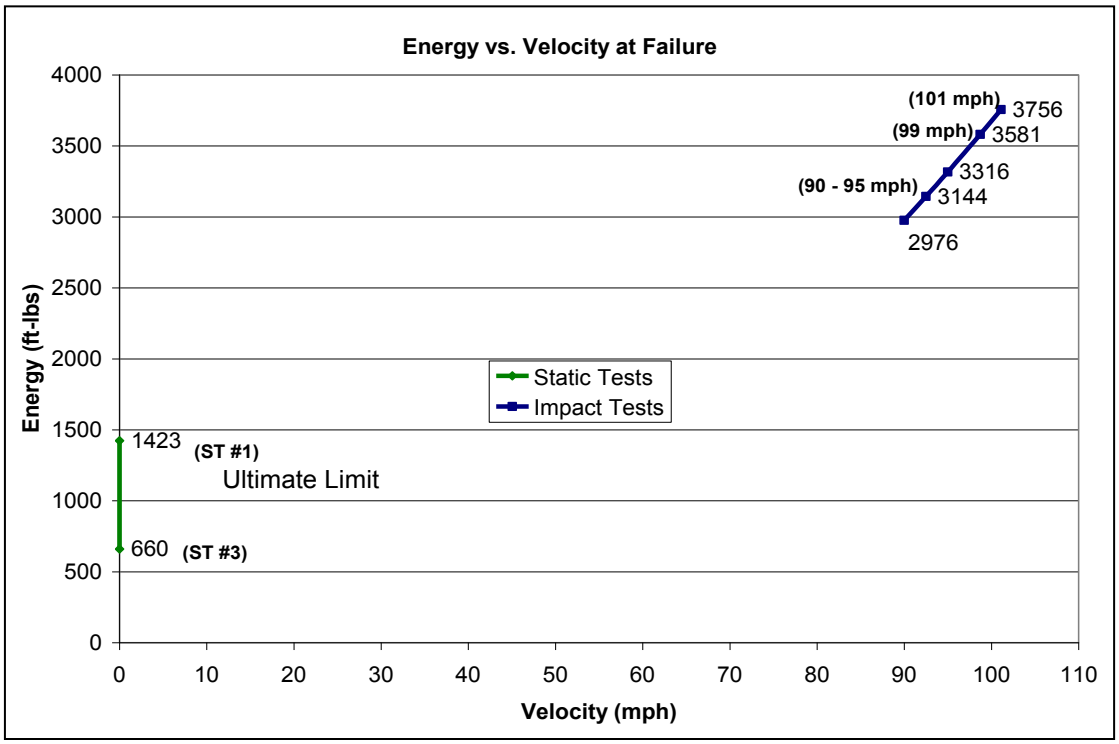

Figure 4.4 Energy vs. Velocity for Specimens at Failure

The statically loaded specimen is not perfectly level at the rear layer, and there may be a small variation in height of the three rollers and the gaps between the boards on the bottom layer of the specimen. This would result in an increased deflection at the lower loads but somewhat linear deflection as the bearing surface became consistently supported.

4.4 Support Variations

Four different support conditions were used. The first support system, which used a rigid wood backing frame (Figure 2.2), proved moderately effective for supporting specimens with elements bending about the strong axis. Though it survived a single shot, it was considerably damaged. As a result, a new support system was developed.

The support system in which two specimens were connected at 90 degrees (orthogonally) proved to be effective in certain situations, and was useful in the design of the final support system. This intermediate support system was sufficiently rigid to test stronger wall designs but resulted in support system failures. For wall designs that resisted penetration, the edge supports failed where fasteners sheared or came loose at both top and bottom supports (Figure 2.6). Although the support system failed in these tests, the results suggested that increased flexibility led to longer impact duration and decreased the overall force on the specimen as well as dissipating the energy towards the middle of the specimen. These results led to another modification and the final support system design.

In order to minimize the effects of the strength (as opposed to flexibility) of the support system, a steel backing frame (Figure 2.5) was constructed on top of a steel turntable (Figure 2.4) that rotated for different impact angles. When specimens were rigidly attached directly to the vertical frame, the tests above 66 and 75 mph (106 and 121 km/h) failed in 45° angle of impact tests. When a flexible backing (1 in. [25 mm] thick Styrofoam) was placed between the specimen and the frame, the specimens not only survived the test at up to 116 mph (187 km/h) (45° angle of impact), but were also in good enough condition to be retested, while the specimens tests at a 90° angle of impact were nearly able to stop the 100 mph (161 km/h) tests. One of the specimens underwent a second test and, although this test was at a higher velocity, it was still in good enough condition for a third test.

As shown in Table 3.3 for rigidly supported specimens, local deflections (maximum centerpoint deflection before edge movement) were significantly larger and were close to global deflections (maximum overall deflection including edge movement) for each test. This suggests that the duration of impact was short, leading to a higher force on the specimen compared with the flexibly supported specimens. Specimens with flexible support had small localized deflections (Table 3.4), which were also significantly smaller than global deflections, suggesting that the whole specimen resisted the load and used the elasticity of the Styrofoam backing to increase duration of impact, thus decreasing the impact force.

A duration of impact less than 6.7 milliseconds resulted in an impact load of 6.2 kips (28 kN) for the flexibly supported, flexibly designed specimens, an impact impact time of sixty milliseconds resulted in an impact force of 60.0 kips (267 kN) (Equation 1.5, Table 1.2), suggesting that up to 53.8 kips (239 kN) was dispersed by the specimen and its support system. It is amazing to see how much kinetic energy can be withstood by a flexible system compared with a rigidly designed structure!

In summary, the use of a flexible backing, as expected, to resist the impact load dramatically increased its ability to pass the test load by increasing the time of impact. The biggest surprise, though, is the effectiveness that a 1 in. (25 mm) thick piece of Styrofoam had in helping the specimens resist the load.

5. SUMMARY

5.1 Conclusions

A number of conclusions can be deduced from this research.

1. The all wood subassemblies consisting of four layers of 1x4s bending about the weak axis, fastened together with screws in the Method 2 direction and the Edge/Cross configuration with flexible supports, show potential to resist hurricane force loads (80 mph [129 km/h]) at hurricane durations (six loadings). For a 90° AOI, the success threshold for a single test is in the 90-95 mph (145-153 km/h) range.

2. The Edge/Cross connection pattern was the most efficient method of those tried in resisting the impact load, while the Method 2 fastener direction are inserted aids in resisting the load.

3. Reducing the angle of impact had a distinct effect on the ability of the specimen to withstand the loading by reducing the load perpendicular to the specimen face.

4. Flexible backing creates a significant increase in specimen success.

5. Impact loaded subassemblies withstood a kinetic impact energy that was 250% to 680% of the amount of energy absorbed by the statically loaded specimens, though it is unknown what effect this has on the wood's ultimate load capacity.

5.2 Recommendations

An interesting observation during testing was that some specimens that either translated and/or rotated due to support failure or were flexibly supported by a backing frame were more likely to survive a shot. This makes sense as the impulse-momentum relationship dictates that a longer duration of impact will give a lower impact force. As such, more studies should be made of walls in which the structure is either flexibly supported or is allowed to move. The type of flexible support can be Styrofoam or the subject of study itself.

As the angle of impact can be crucial to the survival of the structure, one recommendation is towards the development of a structure that approaches a circular shape, such as an octagon, decagon, etc. In addition to the fact that round assemblies distribute loads better than flat ones, a round structure is more likely to have a missile impact one of its walls at an angle, thereby reducing the overall load on the structure.

In addition, finite element modeling should be developed to simulate the static and dynamic tests.

5.3 Future Research

There are many aspects that are involved in the construction of a fully operational storm shelter as provided for in FEMA 361. As this research only entailed a successful subassembly of a maximum size of 4 ft (1.2 m) by 4 ft (1.2 m), studies should be undertaken to test the effect of larger assemblies of the same configuration. Additionally, this entails the connection of multiple walls to form the entire structure, along with the possibility of missile resistant windows, a design for a door, which was discussed in FEMA 361, and the connection of the structure to a foundation. Testing on a wider range of duration of load (i.e., tests between 0.001 seconds and more "static" loads) would provide more useful information as well.

As previously noted, the research into various forms of flexible backing would be interesting and significant, as the use of flexible backing considerably increased the ability of the wall specimens to survive the testing.

An interesting possibility for research comes in the statistical approach to the method at which the loads are applied. A study should investigate the probabilities at which the missile may impact the structure, as a 45° angle of impact reduces impact energy by 50%. Hits at other angles also resulted in lessened loads in impact tests, but to a different extent. A comprehensive study of different angular hits would aid in the research of a round structure by helping to specify how many sides would be optimal for a significant reduction in loads.

If an efficient and inexpensive structure can be designed, an all wood storm shelter/wall assembly may have wide ranging implications. Large walls could be formed and placed into larger walls of critical pieces of infrastructure, such as hospitals. Additionally, if an inexpensive structure can be designed, these shelters can be constructed in developing countries throughout the world to save lives in places with the most need.

REFERENCES

Alciatore, D. "High Speed Camera." Dept. of Mechanical Engineering, Colorado State University, Fort Collins, Colorado. (2009). <http://high_speed_video.colostate.edu/camera.html>.

American Forest and Paper Association (AFPA). *National Design Specification for Wood Construction*. Table 4B. Madison, Wisconsin. (2001).

American Society for Testing and Materials (ASTM) E 1886. Standard Test Method for Performance of Exterior Windows, Curtain Walls, Doors, and Impact Protective Systems Impacted by Missile(s) and Exposed to Cyclic Pressure Differentials. West Conhoshocken, Pennsylvania. (January 2005).

American Society for Testing and Materials (ASTM) E 1996. *Standard Specification for Performance of Exterior Windows, Curtain Walls, Doors and Impact Protective Systems Impacted by Windborne Debris in Hurricanes*. West Conshohocken, Pennsylvania. (April 2009).

Buchar, J., and V. Adamik. "Wood Strength Evaluation." Proceedings of the 39th International Conference on Experimental Stress Analysis 2001. Tabor, Czech Republic, Czech Technical University, Prague. (June 4 -6, 2001).

Colorado State University (CSU) Structures Lab. "Impact Testing of Wood Wall Configurations." Department of Civil and Environmental Engineering, Colorado State University, Ft. Collins, Colorado. (2009). http://www.engr.colostate.edu/StructuresLab/FEMA/index.html

Elmendorf, A. "Stresses in Impact." *Journal of the Franklin Institute* 182, pp 771 to 790. Philadelphia, Pennsylvania. (1916).

Federal Emergency Management Agency (FEMA) 361. *Design and Construction for Community Safe Rooms*. Washington, D.C. (August 2008)

Jansson, B. "Impact Loading of Timber Beams." RILEM Symposium on Timber Engineering. Stockholm, Sweden (September 13-14, 1999).

Kolsky, K. *Stress Waves in Soils*. Dover. New York, New York. (1963).

Liska, J. A. *Effect of Rapid Loading on the Compressive and Flexural Strength of Wood*, United States Department of Agriculture. Forest Products Laboratory.. R1767. Madison, Wisconsin. (1950).

National Oceanic and Atmospheric Administration. "Enhanced F-Scale for Tornado Damage." <http://www.spc.noaa.gov/faq/tornado/ef-scale.html>. (2007).

Richart, F.E., J.R. Hall, and R.D. Woods. *Vibrations of Soils and Foundations*. Prentice Hall, Englewood Cliffs, New Jersey. (1970).

Rinehart, J.S. *Stress Transients in Solids*. Hyperdynamics, Santa Fe, NM. (1975).

Texas Tech University Wind Science and Engineering Research Center. "Summary Report on Debris Impact Testing at Texas Tech University." Department of Civil and Environmental Engineering. Lubbock, Texas. (June 2003).

Timoshenko, S.P. and J.W. Goodier. *Theory of Elasticity*. McGraw-Hill, New York, New York. (1970).

Veyera, G.E. "Transient Porewater Pressure Response and Liquefication in a Saturated Sand," Ph.D. Dissertation, Dept. of Civil Engineering, Colorado State University, Fort Collins, Colorado (Fall 1985).

Wood, L.W. *Relation of Strength of Wood to Duration of Load*. United States Department of Agriculture. Forest Service. R1916. Madison, Wisconsin: USDA (1951).

Zylkowski, S., Z. Martin, Z., and L. Tanner. "Safe Wood Construction for High Wind." The Engineered Wood Association. Tacoma, Washington. (November 2000).

APPENDIX A: ZONE DESIGNATION FOR UNITED STATES

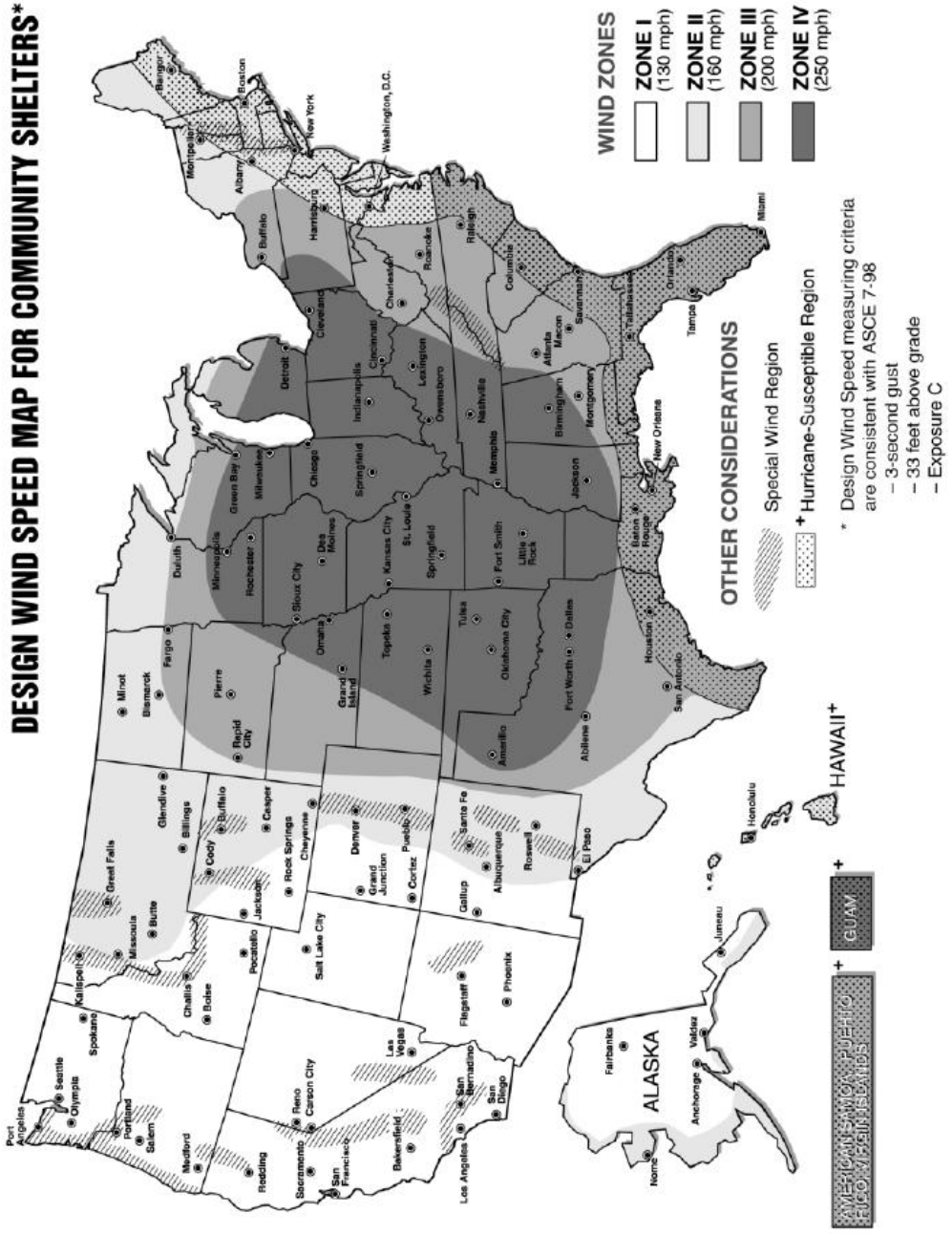

Figure A.1 Wind Speed Designation Map

APPENDIX B: IMPACT TEST CONFIGURATIONS AND RESULTS

APPENDIX C: SAMPLE AND IMPACT LOAD AND ENERGY CALCULATIONS

C.1 Sample Calculations

Equation 1.2

$w = 11 lbs$

$m = \frac{11}{32.2} = 0.34 slugs$

$v = 73.32 mph = 107.54\ ft/s$ From Test #50

$\Delta t = 0.008 \sec$

$F = \frac{0.34 * 107.54}{0.008} * \frac{1 kip}{1000 lbs} = 4.59 kips$

Equation 1.3

$m = 0.34 slugs$

$v = 73.32 mph = 107.54\ ft/s$

$KE = \frac{1}{2} * 0.34 * 107.54^2 = 1975.44\ ft - lbs$

Equations 1.4 – 1.6

$E = 1.585 x 10^8\ psf$

$\rho = 36.83 lb/\ ft^3$

$A = 0.0365\ ft^2$

$v = 73.32 mph = 107.54\ ft/s$

$L = 12\ ft$

$c = \sqrt{\frac{1.585 x 10^8}{36.83}} = 365.58\ ft/s$

$F = 107.54 * 36.83 * 365.58 * 0.0365 = 52.85 kips$

$T_{\max} = \frac{2 * 12}{365.58} = 0.061 \sec$

C.2 45° Angle of Impact Calculations

#	P (psi)	T_0 (sec)	T_1 (sec)	T_2 (sec)	Ref 2"	D_1	D_2	Δ_{Local}	Δ_{Global}	D_0' (in)	D_1' (in)	D_2' (in)
1	105	-0.6137	-0.6113	-0.6100	0.2577	0.3423	0.1875	0.0446	0.1261	2	2.66	1.46
2	100	-0.7350	-0.7327	-0.7307	0.2577	0.3419	0.3087	0.1009	0.1751	2	2.65	2.40
3	150	-0.7927	-0.7910	-0.7893	0.2577	0.3049	0.2948	0.0759	0.1658	2	2.37	2.29
4	150	-0.8203	-0.8180	-0.8153	0.2577	0.3995	0.4577	0.1007	0.1239	2	3.10	3.55
5	270	-0.9810	-0.9797	-0.9783	0.2577	0.3075	0.3281	0.1220	0.1995	2	2.39	2.55
6	350	-1.0593	-1.0583	-1.0573	0.2577	0.2762	0.2527	0.0775	0.1512	2	2.14	1.96
7	270	-0.8110	-0.8093	-0.8080	0.2577	0.3527	0.2963	0.2285	0.5386	2	2.74	2.30
8	350	-0.6897	-0.6887	-0.6873	0.2577	0.2569	0.3475	0.1438	0.2019	2	1.99	2.70
9	350	-0.4253	-0.4243	-0.4233	0.2577	0.2459	0.2588	0.0514	0.1094	2	1.91	2.01

#	T_{impact} (sec)	Δ_{local}' (in)	Δ_{global}' (in)	V_1 (ft/sec)	V_2 (ft/sec)	V_{avg} (ft/sec)	V_{avg} (mph)	m (slugs)	F (kips)	P (ksi)	$F_{45°}$ (kips)	E_{Impact} (ft-lbs)
1	0.007	0.346	0.979	92.24	93.28	92.76	63.25	0.34	4.53	0.86	3.20	1469.75
2	0.0047	0.783	1.359	96.14	99.83	97.98	66.81	0.34	7.12	1.36	5.04	1639.86
3	0.003	0.589	1.287	116.00	112.15	114.07	77.78	0.34	12.99	2.47	9.19	2222.73
4	0.0027	0.782	0.962	112.34	109.64	110.99	75.67	0.34	14.04	2.67	9.93	2104.00
5	0.0037	0.947	1.548	152.98	151.57	152.28	103.82	0.34	14.06	2.68	9.94	3960.63
6	0.0033	0.601	1.173	178.63	163.43	171.03	116.61	0.34	17.71	3.37	12.52	4996.46
7	0.0027	1.773	4.180	134.18	147.41	140.79	96.00	0.34	17.81	3.39	12.60	3385.94
8	0.0024	1.116	1.567	166.15	160.53	163.34	111.37	0.34	23.25	4.43	16.44	4557.17
9	0.0029	0.399	0.849	159.04	167.38	163.21	111.28	0.34	19.23	3.66	13.59	4549.69

C.3 90° Angle of Impact Calculations for Passing Impact Tests

#	P (psi)	T_0 (sec)	T_1 (sec)	T_2 (sec)	Ref 2"	D_1	D_2	D_0' (in)	D_1' (in)	D_2' (in)
1	120	-0.8483	-0.8467	-0.8447	0.3023	0.3299	0.3849	2	2.14	2.49
2	170	-0.6897	-0.6887	-0.6867	0.3089	0.2237	0.4575	2	1.45	2.96
3	120	-0.5717	-0.5700	-0.5683	0.3089	0.3762	0.3863	2	2.44	2.50

T_{impact} (sec)	V_1 (ft/sec)	V_2 (ft/sec)	V_{avg} (ft/sec)	V_{avg} (mph)	m (slugs)	F (kips)	P (ksi)	E_{Impact} (ft-lbs)
0.008	111.25	103.84	107.54	73.32	0.34	4.59	0.87	1975.44
0.0067	120.70	123.42	122.06	83.22	0.34	6.22	1.19	2544.78
0.006	119.40	122.60	121.00	82.50	0.34	6.89	1.31	2500.87

C.4 90° Angle of Impact Calculations for Failing Impact Tests

#	P (psi)	T_0 (sec)	T_1 (sec)	T_2 (sec)	Ref 2"	D_1	D_2
1	*250*	*-0.8447*	*-0.8437*	*-0.8423*	*0.3089*	*0.2632*	*0.3829*
2	*250*	*-0.9297*	*-0.9287*	*-0.9270*	*0.3089*	*0.2752*	*0.4666*
3	170	-0.8727	-0.8713	-0.8693	0.3089	0.2991	0.4427
4	250	-0.9850	-0.9840	-0.9823	0.3089	0.2991	0.4786

D_0' (in)	D_1' (in)	D_2' (in)	V_1 (ft/sec)	V_2 (ft/sec)	V_{avg} (ft/sec)	V_{avg} (mph)
2	*1.70*	*2.48*	*142.01*	*147.57*	***144.79***	*98.72*
2	*1.78*	*3.02*	*148.48*	*148.09*	***148.29***	*101.10*
2	1.94	2.87	115.27	119.43	**117.35**	80.01
2	1.94	3.10	161.38	151.90	**156.64**	106.80